LETTER Communicated by Si Wu

Influence of External Inputs and Asymmetry of Connections on Information-Geometric Measures Involving Up to Ten Neuronal Interactions

Yimin Nie
yimin.nie@uleth.ca
Department of Neuroscience, Canadian Center for Behavioural Neuroscience, University of Lethbridge, Lethbridge, AB T1K 3M4 Canada

Jean-Marc Fellous
fellous@email.arizona.edu
Department of Psychology and Department of Applied Mathematics, University of Arizona, Tucson, AZ 85721, U.S.A.

Masami Tatsuno
tatsuno@uleth.ca
Department of Neuroscience, Canadian Center for Behavioural Neuroscience, University of Lethbridge, Lethbridge, AB T1K 3M4 Canada

The investigation of neural interactions is crucial for understanding information processing in the brain. Recently an analysis method based on information geometry (IG) has gained increased attention, and the property of the pairwise IG measure has been studied extensively in relation to the two-neuron interaction. However, little is known about the property of IG measures involving more neuronal interactions. In this study, we systematically investigated the influence of external inputs and the asymmetry of connections on the IG measures in cases ranging from 1-neuron to 10-neuron interactions. First, the analytical relationship between the IG measures and external inputs was derived for a network of 10 neurons with uniform connections. Our results confirmed that the single and pairwise IG measures were good estimators of the mean background input and of the sum of the connection weights, respectively. For the IG measures involving 3 to 10 neuronal interactions, we found that the influence of external inputs was highly nonlinear. Second, by computer simulation, we extended our analytical results to asymmetric connections. For a network of 10 neurons, the simulation showed that the behavior of the IG measures in relation to external inputs was similar to the analytical solution obtained for a uniformly connected network. When the network size was increased to 1000 neurons, the influence of external inputs almost disappeared. This result suggests that all IG measures from 1-neuron to 10-neuron interactions are robust against the

Neural Computation **26, 2247–2293** (2014)
doi:10.1162/NECO_a_00633

influence of external inputs. In addition, we investigated how the strength of asymmetry influenced the IG measures. Computer simulation of a 1000-neuron network showed that all the IG measures were robust against the modulation of the asymmetry of connections. Our results provide further support for an information-geometric approach and will provide useful insights when these IG measures are applied to real experimental spike data.

1 Introduction

The interaction between neurons plays a key role in information processing in the brain. A number of attempts at understanding the contribution of correlations to information processing have been made by studying pairwise and higher-order neural correlations (Gerstein & Perkel, 1969; Abeles & Gerstein, 1988; Aertsen, Gerstein, Habib, & Palm, 1989; Zhang, Ginzburg, McNaughton, & Sejnowski, 1998; Panzeri & Schultz, 2001; Grün, Diesmann, & Aertsen, 2002a, 2002b; Brown, Kass, & Mitra, 2004; Fellous, Tiesinga, Thomas, & Sejnowski, 2004; Czanner, Grün, & Iyengar, 2005; Shimazaki & Shinomoto, 2007; Amari, 2009; Peyrache, Benchenane, Khamassi, Wiener, & Battaglia, 2009; Shimokawa & Shinomoto, 2009; Lopes-dos-Santos, Conde-Ocazionez, Nicolelis, Ribeiro, & Tort, 2011). Recently information geometry (IG) has provided an information-theoretic approach based on differential geometry and has been used as a powerful tool for analyzing neuronal activity patterns (Amari & Nagaoka, 2000; Amari, 2001; Nakahara & Amari, 2002; Amari, Nakahara, Wu, & Sakai, 2003; Tatsuno & Okada, 2004; Eleuteri, Tagliaferri, & Milano, 2005; Ikeda, 2005; Miura, Okada, & Amari, 2006; Nakahara, Amari, & Richmond, 2006; Tatsuno, Fellous, & Amari, 2009; Ince et al., 2010; Ohiorhenuan & Victor, 2011; Nie & Tatsuno, 2012; Shimazaki, Amari, Brown, & Grün, 2012). The advantages of the IG approach include an orthogonal decomposition of higher-order interactions (Amari, 2001; Nakahara & Amari, 2002; Amari, 2009) and the direct relationship between IG measures and connection weights (Tatsuno & Okada, 2004; Tatsuno et al., 2009; Nie & Tatsuno, 2012).

Many of the previous theoretical studies, including information geometry, have focused on the pairwise interaction or relatively low orders of interactions. However, since the brain may process information with highly coordinated neural activity, the development of a correlation measure that is capable of estimating interactions with more neurons is important. The IG measures are ideal for this purpose because they can be extended to higher-order interactions in a straightforward manner (Amari, 2001). However, a systematic investigation of the relationship between different orders of IG measures and their dependency on network parameters has not yet been conducted. In this study, we investigated how the IG measures derived from up to 10-neuronal interactions were influenced by a correlated input,

a background input, and the asymmetry of connections. First, we derived the analytical relationship between the IG measures and external inputs using a network of 10 neurons that were connected by uniform weights. Second, we extended our investigation to an asymmetrically connected neural network by computer simulation. We investigated how the IG measures were influenced by external inputs and the level of asymmetry of connections.

This study is organized as follows. In section 2, we introduce information geometry, a model network, and a recursive formula for analytically calculating the IG measures. In section 3, we describe the analytical relationship between the IG measures and the external inputs for 10 neurons that are uniformly connected. In section 4, we show the numerical results for an asymmetrically connected neural network of up to 1000 neurons. And in section 5, we summarize the results, discuss the limitations of this work, and propose direction for future studies.

2 Information Geometry, Model Network, and a Recursive Formula for Analytically Calculating the IG Measures

2.1 Information Geometry. In this section, we describe an information-geometric approach (for background, see Amari & Nagaoka, 2000). x_i is a binary variable that represents the state of the ith neuron in cases where it is silent ($x_i = 0$) or produces a spike ($x_i = 1$). $p_{x_1 x_2,\ldots,x_N}$ is the probability of an N-neuron system where we assume $p_{x_1 x_2,\ldots,x_N} > 0$. The full Nth order log-linear model (LLM) of an N-neuron system is given by:

$$\begin{aligned}\log p_{x_1 x_2 \ldots x_N} = &\sum_i \theta_i^{(N,N)} x_i + \sum_{i<j} \theta_{ij}^{(N,N)} x_i x_j + \ldots \\ &+ \sum_{i<j<\cdots<m} \theta_{ij,\ldots,m}^{(N,N)} x_i x_j \ldots x_m \\ &+ \cdots + \theta_{12,\cdots N}^{(N,N)} x_1 x_2 \ldots x_N - \psi(\boldsymbol{\theta})^{(N,N)}, \end{aligned} \tag{2.1}$$

where $\theta_{ij,\ldots,m}^{(N,N)}$ $(1 \le m \le N)$ represents the m-neuron interaction and $\psi(\boldsymbol{\theta})^{(N,N)}$ is the normalizing factor so that $\sum p_{x_1,x_2,\ldots,x_N} = 1$ (Amari & Nagaoka, 2000). The first and second superscripts represent the order of LLM and the number of neurons in the system, respectively. We call $\theta_{ij,\ldots,m}^{(N,N)}$ the m–neuron IG measure of the fully expanded LLM (Tatsuno & Okada, 2004). For simplicity, we also refer to the one-neuron IG measure as the single IG measure and the two-neuron IG measure as the pairwise IG measure. The first few

IG measures and the normalizing factor are expressed as

$$\theta_i^{(N,N)} = \log \frac{p_{x_1=0,\ldots,x_i=1,\ldots,x_N=0}}{p_{x_1=0,\ldots,x_N=0}},$$

$$\theta_{ij}^{(N,N)} = \log \frac{p_{x_1=0,\ldots,x_i=1,\ldots,x_j=1,\ldots,x_N=0}\, p_{x_1=0,\ldots,x_N=0}}{p_{x_1=0,\ldots,x_i=1,\ldots,x_j=0,\ldots,x_N=0}\, p_{x_1=0,\ldots,x_i=0,\ldots,x_j=1,\ldots,x_N=0}},$$

$$\theta_{ijk}^{(N,N)} = \log \frac{p_{x_i=1,x_j=1,x_k=1;x_{N-i,j,k}=0}\, p_{x_i=1;x_{N-i}=0}\, p_{x_j=1;x_{N-j}=0}\, p_{x_k=1;x_{N-k}=0}}{p_{x_i=1,x_j=1;x_{N-i,j}=0}\, p_{x_j=1,x_k=1;x_{N-j,k}=0}\, p_{x_i=1,x_k=1;x_{N-i,k}=0}\, p_{x_{1:N}=0}},$$

$$\begin{aligned}
&\theta_{ijkl}^{(N,N)} \\
&= \log \left(\frac{p_{x_i=1,x_j=1,x_k=1,x_l=1;x_{N-i,j,k,l}=0}\, p_{x_i=1,x_j=1;x_{N-i,j}=0}\, p_{x_i=1,x_k=1;x_{N-i,k}=0}}{p_{x_i=1,x_j=1,x_k=1;x_{N-i,j,k}=0}\, p_{x_i=1,x_j=1,x_l=1;x_{N-i,j,l}=0}\, p_{x_i=1,x_k=1,x_l=1;x_{N-i,k,l}=0}} \right. \\
&\quad \times \frac{p_{x_i=1,x_l=1;x_{N-i,l}=0}\, p_{x_j=1,x_k=1;x_{N-j,k}=0}\, p_{x_j=1,x_l=1;x_{N-j,l}=0}\, p_{x_k=1,x_l=1;x_{N-k,l}=0}}{p_{x_j=1,x_k=1,x_l=1;x_{N-j,k,l}=0}\, p_{x_i=1;x_{N-i}=0}\, p_{x_j=1;x_{N-j}=0}\, p_{x_k=1;x_{N-k}=0}} \\
&\quad \left. \times \frac{p_{x_{1:N}=0}}{p_{x_l=1;x_{N-l}=0}} \right), \\
&\quad \cdots \quad \cdots \quad \cdots \\
&\psi(\boldsymbol{\theta})^{(N,N)} = -\log p_{x_1=0,\ldots,x_N=0}
\end{aligned} \tag{2.2}$$

where $1 \le i < j < k < l \le N$. Note that for $\theta_{ijk}^{(N,N)}$ and $\theta_{ijkl}^{(N,N)}$, we used the following form of representation:

$$\begin{aligned}
p_{x_i=1,x_j=1,x_k=1;x_{N-i,j,k}=0} &= p_{x_1=0,\ldots,x_i=1,\ldots,x_j=1,\ldots,x_k=1,\ldots,x_N=0} \\
p_{x_i=1,x_j=1,x_k=1,x_l=1;x_{N-i,j,k,l}=0} &= p_{x_1=0,\ldots,x_i=1,\ldots,x_j=1,\ldots,x_k=1,\ldots,x_i=1,\ldots,x_N=0}.
\end{aligned} \tag{2.3}$$

In general terms, the partially expanded kth order LLM of an N-neuron system is expressed by

$$\begin{aligned}
\log p_{x_1 x_2 \ldots x_{k*\ldots*}} = &\sum_i \theta_i^{(k,N)} x_i + \sum_{i<j} \theta_{ij}^{(k,N)} x_i x_j \\
&+ \cdots + \sum_{i<j<\cdots<m} \theta_{ij,\ldots,m}^{(k,N)} x_i x_j \ldots x_m \\
&+ \cdots + \theta_{12,\ldots k}^{(k,N)} x_1 x_2 \ldots x_k - \psi(\boldsymbol{\theta})^{(k,N)},
\end{aligned} \tag{2.4}$$

where $\theta^{(k,N)}_{12,\ldots,m}$ $(1 \le m \le k \le N)$ is the m-neuron IG measure of the partially expanded kth order LLM. The first few terms and normalizing factor are given as follows:

$$\theta^{(k,N)}_i = \log \frac{p_{x_1=0,\ldots,x_i=1,\ldots,x_k=0,*\ldots*}}{p_{x_1=0,\ldots,x_k=0,*\ldots*}},$$

$$\theta^{(k,N)}_{ij} = \log \frac{p_{x_1=0,\ldots,x_i=1,\ldots,x_j=1,\ldots,x_k=0,*\ldots*} p_{x_1=0,\ldots,x_k=0,*\ldots*}}{p_{x_1=0,\ldots,x_i=1,\ldots,x_j=0,\ldots,x_k=0,*\ldots*} p_{x_1=0,\ldots,x_i=0,\ldots,x_j=1,\ldots,x_k=0,*\ldots*}},$$

$$\theta^{(k,N)}_{ijq} = \log \frac{p_{x_i=1,x_j=1,x_q=1;x_{k-i,j,q}=0;*} p_{x_i=1;x_{k-i}=0;*} p_{x_j=1;x_{k-j}=0;*} p_{x_q=1;x_{k-q}=0;*}}{p_{x_i=1,x_j=1;x_{k-i,j}=0;*} p_{x_j=1,x_q=1;x_{k-j,q}=0;*} p_{x_i=1,x_q=1;x_{k-i,q}=0;*} p_{x_{1:k}=0;*}},$$

$$\theta^{(k,N)}_{ijqr} =$$

$$\log \left(\frac{p_{x_i=1,x_j=1,x_q=1,x_r=1;x_{k-i,j,q,r}=0;*} p_{x_i=1,x_j=1;x_{k-i,j}=0;*} p_{x_i=1,x_q=1;x_{k-i,q}=0;*}}{p_{x_i=1,x_j=1,x_q=1;x_{k-i,j,q}=0;*} p_{x_i=1,x_j=1,x_r=1;x_{k-i,j,r}=0;*} p_{x_i=1,x_q=1,x_r=1;x_{k-i,q,r}=0;*}} \right.$$

$$\times \frac{p_{x_i=1,x_r=1;x_{k-i,r}=0;*} p_{x_j=1,x_q=1;x_{k-j,q}=0;*} p_{x_j=1,x_r=1;x_{k-j,r}=0;*} p_{x_q=1,x_r=1;x_{k-q,r}=0;*}}{p_{x_j=1,x_q=1,x_r=1;x_{k-j,q,r}=0;*} p_{x_i=1;x_{k-i}=0;*} p_{x_j=1;x_{k-j}=0;*} p_{x_q=1;x_{k-q}=0;*}}$$

$$\left. \times \frac{p_{x_{1:k}=0;*}}{p_{x_r=1;x_{k-r}=0;*}} \right),$$

$$\ldots \quad \ldots \quad \ldots$$

$$\psi(\boldsymbol{\theta})^{(k,N)} = -\log p_{x_1=0,\ldots,x_k=0,*\ldots*}, \tag{2.5}$$

where $*\ldots*$ represents the marginalization over the $(N-k)$ neurons. Also note that for $\theta^{(k,N)}_{ijq}$ and $\theta^{(k,N)}_{ijqr}$, we used the following form of representation:

$$p_{x_i=1,x_j=1,x_q=1;x_{k-i,j,q}=0;*} = p_{x_1=0,\ldots,x_i=1,\ldots,x_j=1,\ldots,x_q=1,\ldots,x_k=0,*\ldots*},$$
$$p_{x_i=1,x_j=1,x_q=1,x_r=1;x_{k-i,j,q,r}=0;*} = p_{x_1=0,\ldots,x_i=1,\ldots,x_j=1,\ldots,x_q=1,\ldots,x_r=1,\ldots,x_k=0,*\ldots*} \tag{2.6}$$

Both $\theta^{(N,N)}_{ij,\ldots,m}$ (the IG measure from the full model) and $\theta^{(k,N)}_{ij,\ldots,m}$ (the IG measure from the kth order partial model) represent the m-neuron interactions. However, note the difference between them: $\theta^{(N,N)}_{ij,\ldots,m}$ is calculated from the full information of all N neurons. By contrast, $\theta^{(k,N)}_{ij,\ldots,m}$ is calculated from the partial information of k neurons by marginalizing $(N-k)$ neurons. It has been shown that $\theta^{(N,N)}_{ij,\ldots,N}$ is statistically orthogonal to any $\langle x_i \rangle$ where $\langle x_i \rangle$ represents the expectation of x_i. On the other hand, $\theta^{(k,N)}_{ij,\ldots,k}$ is orthogonal to $\langle x_i \rangle$

for i that is included in the k neurons (Amari, 2001; Nakahara & Amari, 2002).

To calculate the IG measures, it is often convenient to use the relationship between the marginal and coincident firings ($\langle x_i\rangle, \langle x_i x_j\rangle, \ldots, \langle x_1 x_2 \ldots x_N\rangle$) and the probability of events ($p_{x_1 x_2}, p_{x_1 x_2 x_3} \ldots, p_{x_1 x_2 \ldots x_N}$). For the IG measures with the full LLM, by extending the previous study (Nie & Tatsuno, 2012), we have

$$
\begin{aligned}
p_{x_1=0,\ldots,x_N=0} &= 1-\sum_i \langle x_i\rangle + \sum_{i<j}\langle x_i x_j\rangle - \sum_{i<j<k}\langle x_i x_j x_k\rangle + \cdots \pm \langle x_1 x_2 \ldots x_N\rangle,\\
p_{0,\ldots 0,x_q=1,0\ldots,0} &= \langle x_q\rangle - \sum_{i\neq q}\langle x_q x_i\rangle + \sum_{i,\,j\neq q}\langle x_q x_i x_j\rangle - \cdots \mp \langle x_1 x_2 \ldots x_N\rangle,\\
p_{0,\ldots 0,x_q=1,0\ldots 0,x_r=1,0\ldots,0} &= \langle x_q x_r\rangle - \sum_{i\neq q,r}\langle x_q x_r x_i\rangle + \cdots \pm \langle x_1 x_2 \ldots x_N\rangle,\\
p_{0,\ldots 0,x_q=1,0\ldots 0,x_r=1,0\ldots,0,x_s=1,0\ldots 0} &\\
&= x_q x_r x_s - \sum_{i\neq q,r,s}\langle x_q x_r x_s x_i\rangle + \cdots \mp \langle x_1 x_2 \ldots x_N\rangle,\\
&\quad \cdots \quad \cdots \quad \cdots\\
p_{x_1=1,\ldots,x_N=1} &= \langle x_1 x_2 \ldots x_N\rangle,
\end{aligned}
\tag{2.7}
$$

where an upper sign (lower sign) at the last term on the right-hand side is taken when N is an even (odd) number. Similarly, for the partly expanded kth order IG measures, the formula becomes

$$
\begin{aligned}
p_{x_1=0,\ldots,0,x_k=0,*\ldots*} &= 1 - \sum_{i=1}^{k}\langle x_i\rangle + \sum_{i=1}^{k-1}\sum_{j=i+1}^{k}\langle x_i x_j\rangle - \cdots \pm \langle x_1 x_2 \ldots x_k\rangle,\\
p_{x_1=0,\ldots,0,x_q=1,0\ldots 0,x_k=0,*\ldots*} &\\
&= \langle x_q\rangle - \sum_{i=1,i\neq q}^{k}\langle x_q x_i\rangle + \sum_{i=1,i\neq q}^{k-1}\sum_{j=i+1,\,j\neq q}^{k}\langle x_q x_i x_j\rangle - \cdots \mp \langle x_1 x_2 \ldots x_k\rangle,\\
p_{x_1=0,\ldots,0,x_q=1,0\ldots 0,x_r=1,0\ldots 0,x_k=0,*\ldots*} &= \langle x_q x_r\rangle - \sum_{i=1,i\neq q,r}^{k}\langle x_q x_r x_i\rangle + \cdots \pm \langle x_1 x_2 \ldots x_k\rangle,\\
p_{x_1=0,\ldots,0,x_q=1,0\ldots 0,x_r=1,0\ldots 0,x_s=1,0\ldots 0,x_k=0,*\ldots*} &\\
&= \langle x_q x_r x_s\rangle - \sum_{i=1,i\neq q,r,s}^{k}\langle x_q x_r x_s x_i\rangle + \cdots \mp \langle x_1 x_2 \ldots x_k\rangle,\\
&\quad \cdots \quad \cdots \quad \cdots\\
p_{x_1=1,\ldots,x_k=1,*\ldots*} &= \langle x_1 x_2 \ldots x_k\rangle,
\end{aligned}
\tag{2.8}
$$

where an upper sign (lower sign) at the last term on the right-hand side is taken when k is an even (odd) number.

In summary, the probability of events $(p_{x_1x_2}, p_{x_1x_2x_3}, \ldots, p_{x_1x_2\ldots x_k}, \ldots, p_{x_1x_2\ldots x_N})$ can be calculated from the marginal and coincident firings $(\langle x_i\rangle, \langle x_ix_j\rangle, \ldots, \langle x_1x_2\ldots x_k\rangle, \ldots, \langle x_1x_2\ldots x_N\rangle)$ using equation 2.7 for the full LLM and equation 2.8 for the partially expanded LLM. The IG measures with any neuronal interactions can be then calculated with equation 2.2 for the full LLM and with equation 2.5 for the partially expanded LLM. However, performing these calculations for large N is difficult. In addition, obtaining the relationship between $(\langle x_i\rangle, \langle x_ix_j\rangle, \ldots, \langle x_1x_2\ldots x_k\rangle, \ldots, \langle x_1x_2\ldots x_N\rangle)$ and network parameters such as external inputs for an arbitrary network structure is not straightforward. Therefore, in the analytical part of this study, we focused on a uniformly connected network of 10 neurons. Our goal was to obtain insight into how the IG measures derived from up to 10-neuron interactions were related to external inputs. We also expanded the study to include asymmetric connections and a network with more neurons through the use of computer simulation. In the next section, we describe the structure and dynamics of the neural network that we used in this study.

2.2 Model Network

2.2.1 General Description. We begin with a general description of a network (see Figure 1). The network consists of a layer of recurrently connected N neurons n_i $(i = 1, \ldots, N)$, where a connection strength from a presynaptic neuron (j) to a postsynaptic neuron (i) is represented by J_{ij}. Each neuron in the layer receives a correlated input from a single upstream neuron n_0 with a connection strength represented by W_{i0}. It also receives a background input h_i. The upstream neuron n_0 receives a background input h_0. We assume that a background input is a random variable $h_i \sim N(m_i, \sigma_i)$, where $N(m_i, \sigma_i)$ is the normal distribution with the mean (m_i) and variance (σ_i^2). If we let $x_i(t)$ be the state of the ith neuron at time t, the binary values 0 and 1 correspond to a quiescent and active state, respectively. Under these conditions, the total input to the ith neuron n_i in the layer and to the upstream neuron n_0 is written as follows:

$$u_i(t) = \sum_{j\neq i} J_{ij}x_j(t) + W_{i0}x_0(t) + h_i(t), \tag{2.9}$$

$$u_0(t) = h_0(t). \tag{2.10}$$

The first term on the right-hand side of equation 2.9 represents inputs from the neurons in the same layer. The second and third terms on the right-hand side of equation 2.9 represent a correlated input from the upstream neuron n_0 and uncorrelated background input, respectively.

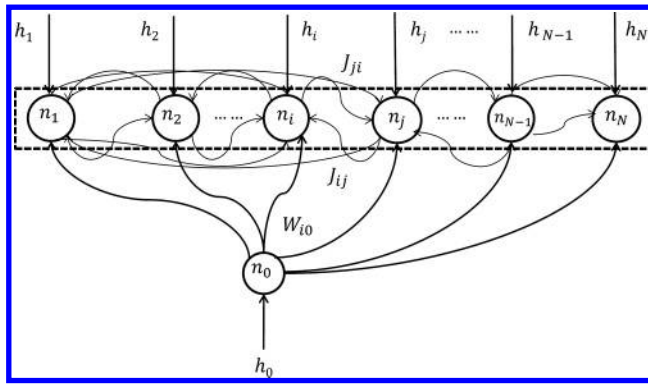

Figure 1: Schematic of a network. Neurons in the upper layer, n_i $(i = 1, \ldots, N)$, are connected by the connection weight J_{ij} from a presynaptic neuron (j) to a postsynaptic neuron (i). Each neuron in the layer receives a correlated input from a single upstream neuron n_0 with a connection strength represented by W_{i0}. It also receives a background input h_i. The upstream neuron n_0 receives a background input h_0. A background input is a random variable $h_i \sim N(m_i, \sigma_i)$ where $N(m_i, \sigma_i)$ is the normal distribution with the mean (m_i) and variance (σ_i^2).

The response of the model neuron is stochastic, depending on the total input u_i. Following the work of Ginzburg and Sompolinsky (1994), we write the transition rate w between the binary states as

$$w\left(x_i \to \left(1 - x_i\right)\right) = \frac{1}{2\tau_0}\left\{1 - \left(2x_i - 1\right)\left[2g(u_i) - 1\right]\right\}, \tag{2.11}$$

where τ_0 is a microscopic characteristic time and $g(u_i)$ is a monotonically increasing sigmoidal function whose value is bounded in the interval [0, 1]. The firing probability of a neuronal state variable $\langle x_i(t)\rangle$ is

$$\tau_0 \frac{d}{dt}\langle x_i(t)\rangle = -\langle x_i(t)\rangle + \langle g(u_i(t))\rangle. \tag{2.12}$$

Note that

$$\langle x_i(t)\rangle = p_{*\ldots*x_i(t)=1*\ldots*} \tag{2.13}$$

is the marginal probability distribution of $x_i(t)$ where the ith neuron takes the value 1, while all the other $N - 1$ neurons take arbitrary values (0 or 1). Similarly, the coincident firing of the ith and jth neurons, $\langle x_i(t)x_j(t)\rangle =$

$p_{*\ldots*,x_i(t)=1,*\ldots*,x_j(t)=1,*\ldots*}$, is expressed as

$$\tau_0 \frac{d}{dt}\langle x_i(t)x_j(t)\rangle = -2\langle x_i(t)x_j(t)\rangle + \langle x_i(t)g(u_j(t))\rangle + \langle x_j(t)g(u_i(t))\rangle. \tag{2.14}$$

The coincident firing of N neurons, $\langle x_1(t)x_2(t)\ldots x_N(t)\rangle = p_{x_1(t)=1,x_2(t)=1,\ldots,x_N(t)=1}$, is written as

$$\begin{aligned}
&\tau_0 \frac{d}{dt}\langle x_1(t)x_2(t)\ldots x_N(t)\rangle \\
&\quad = -N\langle x_1(t)x_2(t)\ldots x_N(t)\rangle + \langle x_2(t)x_3(t)\ldots x_{N-1}(t)x_N(t)g(u_1(t))\rangle \\
&\qquad + \langle x_1(t)x_3(t)\ldots x_{N-1}(t)x_N(t)g(u_2(t))\rangle \\
&\qquad + \cdots + \langle x_1(t)x_2(t)\ldots x_{N-2}(t)x_{N-1}(t)g(u_N(t))\rangle.
\end{aligned} \tag{2.15}$$

For mathematical clarity, we investigate neural interactions when the network is in the equilibrium state. Equations 2.12, 2.14, and 2.15 then reduce to

$$\langle x_i\rangle = \langle g(u_i)\rangle. \tag{2.16}$$

$$\langle x_i x_j\rangle = \frac{1}{2}(\langle x_i g(u_j\rangle) + \langle x_j g(u_i)\rangle), \tag{2.17}$$

$$\begin{aligned}
\langle x_1x_2\ldots x_N\rangle = \frac{1}{N}\big(&\langle x_2x_3\ldots x_{N-1}x_N g(u_1)\rangle \\
&+ \langle x_1x_3\ldots x_{N-1}x_N g(u_2)\rangle \\
&+ \cdots + \langle x_1x_2\ldots x_{N-2}x_{N-1}g(u_N)\rangle\big).
\end{aligned} \tag{2.18}$$

Note that $\langle x_i\rangle = p_{*\ldots*,x_i=1,*\ldots*}$, $\langle x_i x_j\rangle = p_{*\ldots*,x_i=1,*\ldots*,x_j=1,*\ldots*}$ and $\langle x_1x_2\ldots x_N\rangle = p_{x_1=1,x_2=1,\ldots,x_N=1}$ do not depend on t.

2.2.2 Simplified Network. Our goal for the analytical part of this study is to find the explicit relationship between $(\langle x_i\rangle, \langle x_i x_j\rangle, \ldots, \langle x_1x_2\ldots x_N\rangle, \ldots, \langle x_1x_2\ldots x_N\rangle)$ in equations 2.16, 2.17, and 2.18 and external inputs (a correlated input W_{i0} and a background input h_i). To help facilitate the analytical investigation, we set all recurrent connections to be equal (uniform): $J_{ij} = J$. In addition, for mathematical clarity, we assumed that a connection weight from the upstream neuron (n_0) to a neuron (n_i) is uniform and that the background input to a neuron (n_i) has the same mean (h) and variance σ^2

($h_i \sim N(h, \sigma)$). These assumptions simplified equation 2.9 as follows:

$$u_i(t) = J \sum_{j \neq i} x_j(t) + W x_0(t) + h_i(t). \tag{2.19}$$

For a sigmoidal activation function $g(u_i)$, we used:

$$g(u_i) = \frac{1 + \tanh(u_i - m)}{2}, \tag{2.20}$$

where m is a parameter controlling the firing probability of a model neuron.

In the equilibrium limit, the influence of the background input is characterized by its mean value h. In the following section, we investigate how the strength of a correlated input (W) and the mean of a background input (h) influence the IG measures.

2.3 Derivation of System Equations in the Equilibrium Limit

2.3.1 Two-Neuron System. Before we investigate the 10-neuron network, it is instructive to consider a simpler case where the layer contains only 2 neurons. In the equilibrium limit, equation 2.16 for the 2 neurons in the layer is written as

$$\langle x_1 \rangle = \langle g(u_1) \rangle = \langle g(J x_2 + W x_0 + h) \rangle, \tag{2.21}$$

$$\langle x_2 \rangle = \langle g(u_2) \rangle = \langle g(J x_1 + W x_0 + h) \rangle. \tag{2.22}$$

By taking advantage of the relationship,

$$\begin{aligned} g(J x_j + W x_0 + h) = {} & x_0 x_j g(J + W + h) + x_j (1 - x_0) g(J + h) \\ & + (1 - x_j) x_0 g(W + h) + (1 - x_j)(1 - x_0) g(h), \end{aligned} \tag{2.23}$$

and considering $\langle x_1 \rangle = \langle x_2 \rangle$, $\langle x_0 x_1 \rangle = \langle x_0 x_2 \rangle$, equations 2.21 and 2.22 reduce to one equation:

$$\begin{aligned} \langle x_1 \rangle = {} & \langle x_0 x_1 \rangle \{ g(J + W + h) - g(W + h) - (g(J + h) - g(h)) \} \\ & + \langle x_1 \rangle \{ g(J + h) - g(h) \} + \langle x_0 \rangle \{ g(W + h) - g(h) \} + g(h). \end{aligned} \tag{2.24}$$

For an upstream neuron x_0, we have

$$\langle x_0 \rangle = g(h_0). \tag{2.25}$$

For the joint firing of two neurons, equation 2.17 becomes:

$$\begin{aligned}\langle x_1 x_2 \rangle &= \frac{1}{2}[(\langle x_0 x_1 \rangle + \langle x_0 x_2 \rangle)\{g(J+W+h) - g(J+h)\} \\ &\quad + (\langle x_1 \rangle + \langle x_2 \rangle) g(J+h)], \end{aligned} \tag{2.26}$$

$$\langle x_0 x_1 \rangle = \frac{1}{2}[\langle x_0 x_2 \rangle \{g(J+W+h) - g(W+h)\} + \langle x_0 \rangle g(W+h) + \langle x_1 \rangle g(h)], \tag{2.27}$$

$$\langle x_0 x_2 \rangle = \frac{1}{2}[\langle x_0 x_1 \rangle \{g(J+W+h) - g(W+h)\} + \langle x_0 \rangle g(W+h) + \langle x_2 \rangle g(h)]. \tag{2.28}$$

Considering $\langle x_1 \rangle = \langle x_2 \rangle$, $\langle x_0 x_1 \rangle = \langle x_0 x_2 \rangle$, equations 2.27 and 2.28 become identical. Therefore, equations 2.26, 2.27, and 2.28 reduce to two equations:

$$\langle x_1 x_2 \rangle = \langle x_1 x_0 \rangle \{g(J+W+h) - g(J+h)\} + \langle x_1 \rangle g(J+h), \tag{2.29}$$

$$\langle x_0 x_1 \rangle = \frac{1}{2}[\langle x_0 x_1 \rangle \{g(J+W+h) - g(W+h)\} + \langle x_0 \rangle g(W+h) + \langle x_1 \rangle g(h)]. \tag{2.30}$$

For the coincident firing of three neurons, equation 2.18 translates to

$$\begin{aligned}\langle x_0 x_1 x_2 \rangle &= \frac{1}{3}[(\langle x_0 x_1 \rangle + \langle x_0 x_2 \rangle) g(J+W+h) + \langle x_1 x_2 \rangle g(h_0)] \\ &= \frac{1}{3}[2\langle x_0 x_1 \rangle g(J+W+h) + \langle x_1 x_2 \rangle g(h_0)]. \end{aligned} \tag{2.31}$$

Note that we used $\langle x_0 x_1 \rangle = \langle x_0 x_2 \rangle$ from the first to the second lines on the right-hand side of the equation.

We now have five equations (2.24, 2.25, 2.29, 2.30, and 2.31) for five marginal and coincident firings ($\langle x_0 \rangle$, $\langle x_1 \rangle$, $\langle x_0 x_1 \rangle$, $\langle x_1 x_2 \rangle$, and $\langle x_0 x_1 x_2 \rangle$). By solving these equations simultaneously, we represent the marginal and coincident firings in terms of the network parameters J, W, h, h_0, and m. We then use these parameters in equations 2.7 or 2.8 to obtain the probability of events such as p_{x_0}, $p_{x_0 x_1}$, ..., $p_{x_0 x_1 x_2}$. Finally, the IG measures for the full LLM are calculated by using equation 2.2, and the IG measures for the partially expanded LLM are calculated by using equation 2.5.

In the following section, we use a simplified notation such as $\langle x_1 x_2 \rangle$ for $\langle x_i x_j \rangle$ and $\theta_{12}^{(k,N)}$ for $\theta_{ij}^{(k,N)}$ because all IG measures of the same order in the layer are identical due to the uniform connection assumption.

2.3.2 Ten-Neuron System. The equations for a 10-neuron system can be obtained by expanding the procedure in the previous section. Therefore, we solved 21 equations simultaneously for the following 21 marginal and coincident firings: $\langle x_0 \rangle$, $\langle x_1 \rangle$, $\langle x_0 x_1 \rangle$, $\langle x_1 x_2 \rangle$, $\langle x_0 x_1 x_2 \rangle$, $\langle x_1 x_2 x_3 \rangle$, $\langle x_0 x_1 x_2 x_3 \rangle$, $\langle x_1 x_2 x_3 x_4 \rangle$, $\langle x_0 x_1 x_2 x_3 x_4 \rangle$, $\langle x_1 x_2 x_3 x_4 x_5 \rangle$, $\langle x_0 x_1 x_2 x_3 x_4 x_5 \rangle$, $\langle x_1 x_2 x_3 x_4 x_5 x_6 \rangle$, $\langle x_0 x_1 x_2 x_3 x_4 x_5 x_6 \rangle$, $\langle x_1 x_2 x_3 x_4 x_5 x_6 x_7 \rangle$, $\langle x_0 x_1 x_2 x_3 x_4 x_5 x_6 x_7 \rangle$, $\langle x_1 x_2 x_3 x_4 x_5 x_6 x_7 x_8 \rangle$, $\langle x_0 x_1 x_2 x_3 x_4 x_5 x_6 x_7 x_8 \rangle$, $\langle x_1 x_2 x_3 x_4 x_5 x_6 x_7 x_8 x_9 \rangle$, $\langle x_0 x_1 x_2 x_3 x_4 x_5 x_6 x_7 x_8 x_9 \rangle$, $\langle x_1 x_2 x_3 x_4 x_5 x_6 x_7 x_8 x_9 x_{10} \rangle$, and $\langle x_0 x_1 x_2 x_3 x_4 x_5 x_6 x_7 x_8 x_9 x_{10} \rangle$. Since space does not allow us to write all 21 equations, we provide an equation for the first-order marginal $\langle x_1 \rangle$ as an example in the appendix.

Next, we analytically calculated the IG measures with all possible neuronal interactions: the 1-neuron IG ($\theta_1^{(1,10)} - \theta_1^{(10,10)}$), the 2-neuron IG ($\theta_{12}^{(2,10)} - \theta_{12}^{(10,10)}$), the 3-neuron IG ($\theta_{123}^{(3,10)} - \theta_{123}^{(10,10)}$), the 4-neuron IG ($\theta_{1234}^{(4,10)} - \theta_{1234}^{(10,10)}$), the 5-neuron IG ($\theta_{12345}^{(5,10)} - \theta_{12345}^{(10,10)}$), the 6-neuron IG ($\theta_{123456}^{(6,10)} - \theta_{123456}^{(10,10)}$), the 7-neuron IG ($\theta_{1234567}^{(7,10)} - \theta_{1234567}^{(10,10)}$), the 8-neuron IG ($\theta_{12345678}^{(8,10)} - \theta_{12345678}^{(10,10)}$), the 9-neuron IG ($\theta_{123456789}^{(9,10)} - \theta_{123456789}^{(10,10)}$), and the 10-neuron IG ($\theta_{12345678910}^{(10,10)}$). To this end, we took advantage of a simplified network structure where equation 2.2 for the full LLM reduces to

$$\theta_{123\ldots(2s)}^{(N,N)} = \log \frac{p_{\underbrace{1\ldots1}_{2s}\cdot\underbrace{0\ldots0}_{N-2s}} \cdot p_{\underbrace{1\ldots1}_{2s-2}00\cdot\underbrace{0\ldots0}_{N-2s}}^{\binom{2s}{2}} \cdot p_{\underbrace{1\ldots1}_{2s-4}0000\cdot\underbrace{0\ldots0}_{N-2s}}^{\binom{2s}{4}} \cdots p_{\underbrace{0\ldots0}_{N}}}{p_{\underbrace{1\ldots1}_{2s-1}0\cdot\underbrace{0\ldots0}_{N-2s}}^{\binom{2s}{1}} \cdot p_{\underbrace{1\ldots1}_{2s-3}000\cdot\underbrace{0\ldots0}_{N-2s}}^{\binom{2s}{3}} \cdots p_{\underbrace{10\ldots0}_{2s-1}\cdot\underbrace{0\ldots0}_{N-2s}}^{\binom{2s}{1}}}, \tag{2.32}$$

$$\theta_{123\ldots(2s+1)}^{(N,N)} = \log \left(\frac{p_{\underbrace{1\ldots1}_{2s+1}\cdot\underbrace{0\ldots0}_{N-(2s+1)}} \cdot p_{\underbrace{1\ldots1}_{2s-1}00\cdot\underbrace{0\ldots0}_{N-(2s+1)}}^{\binom{2s+1}{2}}}{p_{\underbrace{1\ldots1}_{2s}0\cdot\underbrace{0\ldots0}_{N-(2s+1)}}^{\binom{2s+1}{1}} p_{\underbrace{1\ldots1}_{2s-2}000\cdot\underbrace{0\ldots0}_{N-(2s+1)}}^{\binom{2s+1}{3}}} \times \frac{p_{\underbrace{1\ldots1}_{2s-3}0000\cdot\underbrace{0\ldots0}_{N-(2s+1)}}^{\binom{2s+1}{4}} \cdots p_{\underbrace{0\ldots0}_{2s}\cdot\underbrace{0\ldots0}_{N-(2s+1)}}^{\binom{2s+1}{1}}}{p_{\underbrace{1\ldots1}_{2s-4}000\cdot\underbrace{0\ldots0}_{N-(2s+1)}}^{\binom{2s+1}{5}} \cdots p_{\underbrace{0\ldots0}_{N}}} \right) \tag{2.33}$$

where s is the integer and $\binom{n}{k}$ represents a binomial coefficient. Note that $p_{x_1 \ldots x_{2s+1} \cdot x_{2s+2} \ldots x_N}{}^{\binom{2s+1}{i}}$ expresses possible combinations on the first $(2s+1)$ variables. Similarly, equation 2.5 for the partial LLM reduces to

$$\theta^{(k,N)}_{123\ldots(2s)} = \log\left(\frac{p_{\underbrace{1\ldots1}_{2s}\cdot\underbrace{0\ldots0}_{k-2s}\cdot\underbrace{*\ldots*}_{N-k}}{}^{\binom{2s}{2}} \cdot p_{\underbrace{1\ldots1}_{2s-2}\underbrace{00}\cdot\underbrace{0\ldots0}_{k-2s}\cdot\underbrace{*\ldots*}_{N-k}}{}^{\binom{2s}{2}}}{p_{\underbrace{1\ldots1}_{2s-1}\underbrace{0}\cdot\underbrace{0\ldots0}_{k-2s}\cdot\underbrace{*\ldots*}_{N-k}}{}^{\binom{2s}{1}} \cdot p_{\underbrace{1\ldots1}_{2s-3}\underbrace{000}\cdot\underbrace{0\ldots0}_{k-2s}\cdot\underbrace{*\ldots*}_{N-k}}{}^{\binom{2s}{3}}} \times \frac{p_{\underbrace{1\ldots1}_{2s-4}\underbrace{0000}\cdot\underbrace{0\ldots0}_{k-2s}\cdot\underbrace{*\ldots*}_{N-k}}{}^{\binom{2s}{4}} \cdots p_{\underbrace{0\ldots0}_{k}\cdot\underbrace{*\ldots*}_{N-k}}}{p_{\underbrace{1\ldots1}_{2s-5}\underbrace{000}\cdot\underbrace{0\ldots0}_{k-2s}\cdot\underbrace{*\ldots*}_{N-k}}{}^{\binom{2s}{5}} \cdots p_{1\underbrace{0\ldots0}_{2s-1}\cdot\underbrace{0\ldots0}_{k-2s}\cdot\underbrace{*\ldots*}_{N-k}}{}^{\binom{2s}{1}}} \right) \tag{2.34}$$

$$\theta^{(k,N)}_{123\ldots(2s+1)} = \log\left(\frac{p_{\underbrace{1\ldots1}_{2s+1}\cdot\underbrace{0\ldots0}_{k-(2s+1)}\cdot\underbrace{*\ldots*}_{N-k}}{}^{\binom{2s+1}{2}} \cdot p_{\underbrace{1\ldots1}_{2s-1}\underbrace{00}\cdot\underbrace{0\ldots0}_{k-(2s+1)}\cdot\underbrace{*\ldots*}_{N-k}}{}^{\binom{2s+1}{2}}}{p_{\underbrace{1\ldots1}_{2s}\underbrace{0}\cdot\underbrace{0\ldots0}_{k-(2s+1)}\cdot\underbrace{*\ldots*}_{N-k}}{}^{\binom{2s+1}{1}} \cdot p_{\underbrace{1\ldots1}_{2s-2}\underbrace{000}\cdot\underbrace{0\ldots0}_{k-(2s+1)}\cdot\underbrace{*\ldots*}_{N-k}}{}^{\binom{2s+1}{3}}} \times \frac{p_{\underbrace{1\ldots1}_{2s-3}\underbrace{0000}\cdot\underbrace{0\ldots0}_{k-(2s+1)}\cdot\underbrace{*\ldots*}_{N-k}}{}^{\binom{2s+1}{4}} \cdots p_{1\underbrace{0\ldots0}_{2s}\cdot\underbrace{0\ldots0}_{k-(2s+1)}\cdot\underbrace{*\ldots*}_{N-k}}{}^{\binom{2s+1}{1}}}{p_{\underbrace{1\ldots1}_{2s-4}\underbrace{000}\cdot\underbrace{0\ldots0}_{k-(2s+1)}\cdot\underbrace{*\ldots*}_{N-k}}{}^{\binom{2s+1}{5}} \cdots p_{\underbrace{0\ldots0}_{k}\cdot\underbrace{*\ldots*}_{N-k}}} \right) \tag{2.35}$$

In the next section, we describe how W (the strength of a correlated input to neurons in the layer) and h (the mean of a background input to the neurons in the layer) influence the IG measures using a simplified 10-neuron network.

3 Analytical Study of IG Measures by Uniformly Connected Ten Neurons

In the analytical study in this section, we vary the strength of the correlated input W between 0 and $5J$ where J is the strength of the intrinsic connection between neurons in a layer. J is set to $1/10$ following the general scaling rule of $J = 1/N$ where N is the number of neurons. The range of values is chosen to cover the strength of correlated inputs that could be observed in the brain. For example, the mossy fiber from the dentate gyrus to the CA3 region of the hippocampus is known to make a very strong synaptic connection. This

strength has been estimated to be 5- to 10-fold of the intrinsic recurrent connections in CA3 (Urban, Henze, & Barrionuevo, 2001). Therefore, $W = [0, 50J]$ is wide enough to cover the vast majority of correlated inputs that could be observed experimentally. The strength of the mean background input h is varied between 0 and $5J$. The difference of the range between W and h comes from the different implementation of these inputs. While the correlated input W was modeled with an upstream neuron n_0, the background input h was implemented as a direct input to each neuron in a layer (see equation 2.19). This was done so that the model was consistent with previous studies (Ginzburg & Sompolinsky, 1994; Tatsuno & Okada, 2004; Tatsuno et al., 2009; Nie & Tatsuno, 2012). The parameter m that controls the firing probability of a model neuron in equation 2.24 was set to 1. It corresponds to the firing probability of approximately 0.15 when the network receives the weakest inputs $(W = 0, h = 0)$ and approximately 0.64 when the network receives the maximum inputs $(W = 50J, h = 5J)$.

In the following section, we summarize the results in four categories of the IG measures: the IG measure for a single neuron ($\theta_1^{(k,10)}$), the IG measure for a 2-neuron interaction ($\theta_{12}^{(k,10)}$), the IG measures for 3- to 5-neuron interactions ($\theta_{123}^{(k,10)}$, $\theta_{1234}^{(k,10)}$, $\theta_{12345}^{(k,10)}$), and the IG measures for 6- to 10-neuron interactions ($\theta_{123456}^{(k,10)}$, $\theta_{1234567}^{(k,10)}$, $\theta_{12345678}^{(k,10)}$, $\theta_{123456789}^{(k,10)}$, $\theta_{12345678910}^{(10,10)}$).

3.1 The IG Measure for a Single Neuron Interaction, $\boldsymbol{\theta_1^{(k,10)}}$. The IG measure for a single neuron is the coefficient $\theta_i^{(N,N)}$ in the full LLM (see equation 2.1) and $\theta_i^{(k,N)}$ in the partially expanded LLM (see equation 2.4). Under the condition that there is no correlated input ($W = 0$), a previous study (Tatsuno et al., 2009) showed that $\theta_i^{(2,N)}$ can be related to an uncorrelated background input h_i such as

$$\theta_i^{(2,N)} \propto 2\left(h_i - m\right) + O\left(\frac{1}{N}\right). \tag{3.1}$$

Below, we investigate the influence of a correlated input W and the mean of a background input h to $\theta_i^{(k,N)}$ where k is systematically varied from 1 to 10. For a simplified 10-neuron network, $\theta_i^{(k,N)}$ reduces to $\theta_1^{(k,N)}$, and is given by

$$\theta_1^{(N,N)} = \log \frac{p_{1\cdot 000000000}}{p_{0\cdot 000000000}}, \qquad \left(Full\ LLM\right) \tag{3.2}$$

$$\theta_1^{(k,N)} = \log \frac{p_{1\cdot \underbrace{0\ldots0}_{k-1}\cdot \underbrace{*\ldots*}_{10-k}}}{p_{0\cdot \underbrace{0\ldots0}_{k-1}\cdot \underbrace{*\ldots*}_{10-k}}}. \qquad \left(Partial\ LLM\right) \tag{3.3}$$

Figure 2A shows how $\theta_1^{(k,10)}$ is influenced by a correlated input W in the absence of a background input h (data with a background input are not shown because the overall tendency is the same). The calculation shows that $\theta_1^{(k,10)}$ is linearly related to the strength of W initially but that it becomes insensitive to it (asymptotic flat line). In addition, the influence of W was decreased with the increase of the order of LLM. In contrast, we found that a background input h was related to $\theta_1^{(k,10)}$ linearly regardless of the existence of W (see Figure 2B for $W = 0$, data where $W \neq 0$ were not shown because the overall tendency was same). Furthermore, the figures showed that the linear relationship between $\theta_1^{(k,10)}$ and h described in equation 3.1 holds more strongly for the higher-order LLM, the exact relationship $\theta_1^{(10,10)} = 2(h - m)$ being obtained at $k = 10$ (full LLM; see Figure 2B). In summary, the analytical calculation shows that the single IG measure $\theta_1^{(k,10)}$ is not sensitive to the strength of a correlated input W, but that it is linearly related to the strength of the background input h. In practice, this property could be useful to estimate the relative amount of background input that a neuron receives.

3.2 The IG Measure for a Two-neuron Interaction, $\boldsymbol{\theta_{12}^{(k,10)}}$. The IG measure for a two-neuron interaction $\theta_{ij}^{(k,N)}$ has been extensively studied (Amari, 2001). It has been shown that the measure is statistically independent from firing rate modulation (Nakahara & Amari, 2002; Amari, 2009). Under the assumption that there is no correlated input ($W = 0$), it has also been shown that it is directly related to the sum of connection weights (Tatsuno et al., 2009),

$$\theta_{ij}^{(2,N)} \propto \left(J_{ij} + J_{ji}\right) + O\left(\frac{1}{N}\right), \qquad (Asymmetric\ connection) \tag{3.4}$$

$$\theta_{ij}^{(2,N)} \propto 2J_{ij} + O\left(\frac{1}{N}\right). \qquad (Symmetric\ connection) \tag{3.5}$$

Furthermore, even under the influence of a correlated input W, it has been shown that the pairwise measure with the fourth- or fifth-order LLM, $\theta_{ij}^{(4,N)}$ or $\theta_{ij}^{(5,N)}$, is able to estimate the connection weight provided that the size of the network is sufficiently large ($N = 10^3 - 10^4$) (Nie & Tatsuno, 2012).

For the simplified 10-neuron network, the pairwise IG measure is calculated as

$$\theta_{12}^{(N,N)} = \log \frac{p_{11\cdot 00000000}\, p_{00\cdot 00000000}}{p_{10\cdot 00000000}\, p_{01\cdot 00000000}}, \qquad (Full\ LLM) \tag{3.6}$$

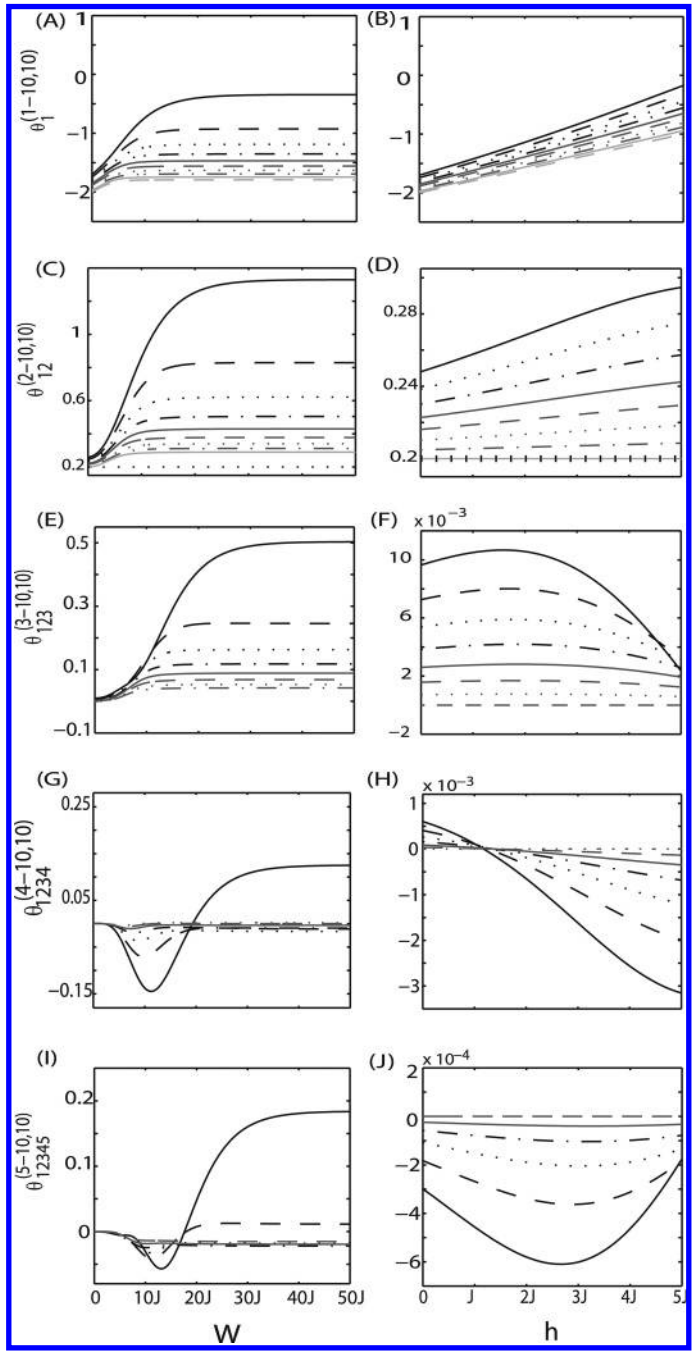
(A)
(B)
(C)
(D)
(E)
(F)
(G)
(H)
(I)
(J)
$\theta_1^{(1-10,10)}$
$\theta_{12}^{(2-10,10)}$
$\theta_{123}^{(3-10,10)}$
$\theta_{1234}^{(4-10,10)}$
$\theta_{12345}^{(5-10,10)}$
x 10^-3
x 10^-4
0 10J 20J 30J 40J 50J
W
0 J 2J 3J 4J 5J
h

$$\theta_{12}^{(k,N)} = \log \frac{p_{11\underbrace{0\ldots0}_{k-2}\cdot\underbrace{*\ldots*}_{10-k}} p_{00\underbrace{0\ldots0}_{k-2}\cdot\underbrace{*\ldots*}_{10-k}}}{p_{10\underbrace{0\ldots0}_{k-2}\cdot\underbrace{*\ldots*}_{10-k}} p_{01\underbrace{0\ldots0}_{k-2}\cdot\underbrace{*\ldots*}_{10-k}}}. \qquad (Partial\ LLM) \tag{3.7}$$

Here, we analytically investigated the influence of a correlated input W and a background input h on $\theta_{12}^{(k,10)}$ where k was systematically varied

Figure 2: Relationship between the IG measures ($\theta_1^{(k,10)}$, $\theta_{12}^{(k,10)}$, $\theta_{123}^{(k,10)}$, $\theta_{1234}^{(k,10)}$, $\theta_{12345}^{(k,10)}$), a correlated input (W), and a background input (h) for a 10-neuron uniformly connected network. The network parameters are set as$J = 1/10$ and $h_0 = 0.5$. W is modified in the range of $[0, 50J]$, and h is modified in the range of $[0, 5J]$. (A) $\theta_1^{(k,10)}$ when a correlated input (W) is varied in the absence of a background input ($h = 0$). (B) $\theta_1^{(k,10)}$ when background input (h) is varied in the absence of a correlated input ($W = 0$). $\theta_1^{(1,10)}$, $\theta_1^{(2,10)}$, $\theta_1^{(3,10)}$, $\theta_1^{(4,10)}$, $\theta_1^{(5,10)}$, $\theta_1^{(6,10)}$, $\theta_1^{(7,10)}$, $\theta_1^{(8,10)}$, $\theta_1^{(9,10)}$, and $\theta_1^{(10,10)}$ are represented by a black solid line, a black dashed line, a black dotted line, a black dash-dot line, a gray solid line, a gray dashed line, a gray dotted line, a gray dash-dot line, a light gray solid line, and a light gray dashed line. (C) $\theta_{12}^{(k,10)}$when a correlated input (W) is varied in the absence of a background input ($h = 0$). (D) $\theta_{12}^{(k,10)}$ when a background input (h) is varied in the absence of a correlated input ($W = 0$). $\theta_{12}^{(2,10)}$, $\theta_{12}^{(3,10)}$, $\theta_{12}^{(4,10)}$, $\theta_{12}^{(5,10)}$, $\theta_{12}^{(6,10)}$, $\theta_{12}^{(7,10)}$, $\theta_{12}^{(8,10)}$, $\theta_{12}^{(9,10)}$, and $\theta_{12}^{(10,10)}$ are represented by a black solid line, a black dashed line, a black dotted line, a black dash-dot line, a gray solid line, a gray dashed line, a gray dotted line, a gray dash-dot line, and a light gray solid line. (E) $\theta_{123}^{(k,10)}$when a correlated input (W) is varied in the absence of a background input ($h = 0$). (F) $\theta_{123}^{(k,10)}$ when a background input (h) is varied in the absence of a correlated input ($W = 0$). $\theta_{123}^{(3,10)}$, $\theta_{123}^{(4,10)}$, $\theta_{123}^{(5,10)}$, $\theta_{123}^{(6,10)}$, $\theta_{123}^{(7,10)}$, $\theta_{123}^{(8,10)}$, $\theta_{123}^{(9,10)}$, and $\theta_{123}^{(10,10)}$ are represented by a black solid line, a black dashed line, a black dotted line, a black dash-dot line, a gray solid line, a gray dashed line, a gray dotted line, and a gray dash-dot line. (G) $\theta_{1234}^{(k,10)}$ when a correlated input (W) is varied in the absence of a background input ($h = 0$). (H) $\theta_{1234}^{(k,10)}$ when a background input (h) is varied in the absence of a correlated input ($W = 0$). $\theta_{1234}^{(4,10)}$, $\theta_{1234}^{(5,10)}$, $\theta_{1234}^{(6,10)}$, $\theta_{1234}^{(7,10)}$, $\theta_{1234}^{(8,10)}$, $\theta_{1234}^{(9,10)}$, and $\theta_{1234}^{(10,10)}$ are represented by a black solid line, a black dashed line, a black dotted line, a black dash-dot line, a gray solid line, a gray dashed line, and a gray dotted line. (I) $\theta_{12345}^{(k,10)}$when a correlated input (W) is varied in the absence of a background input ($h = 0$). (J) $\theta_{12345}^{(k,10)}$ when a background input (h) is varied in the absence of a correlated input ($W = 0$). $\theta_{12345}^{(5,10)}$, $\theta_{12345}^{(6,10)}$, $\theta_{12345}^{(7,10)}$, $\theta_{12345}^{(8,10)}$, $\theta_{12345}^{(9,10)}$, and $\theta_{12345}^{(10,10)}$ are represented by a black solid line, a black dashed line, a black dotted line, a black dash-dot line, a gray solid line, and a gray dashed line.

from 2 to 10. When W was modified, $\theta_{12}^{(k,10)}$ was affected, but to a lesser extent for higher-order k of the LLM (see Figure 2C). Interestingly, when a background input existed, $\theta_{12}^{(k,10)}$ was less likely to be affected by the correlated input (data not shown). Note that $\theta_{12}^{(k,10)} = 0.2 = 2J$ is the correct answer for estimating the sum of the connection weights (a horizontal dashed line). When h was modified, $\theta_{12}^{(k,10)}$ was weakly affected when there was no correlated input (see Figure 2D). For the full LLM ($k = 10$), $\theta_{12}^{(k,10)}$ was completely independent of the modulation of h, providing the correct answer of 0.2 ($2J = 0.2$, the horizontal dashed line). When a correlated input existed, the value of $\theta_{12}^{(k,10)}$ was affected more severely, especially when the order of LLM k was low (data not shown).

In summary, the analysis shows that the pairwise IG measure $\theta_{12}^{(k,10)}$ is a good estimator of the sum of connection weights, even under the influence of both a correlated input W and a background input h. This is especially true if the order of LLM k is high. In practice, the calculation of $\theta_{12}^{(10,10)}$ might not be easy to obtain because of the limited size of experimental data. However, as we previously discussed, $\theta_{12}^{(4,N)}$ or $\theta_{12}^{(5,N)}$ would provide a reasonable estimation of connection weights provided that the size of the network is large (e.g., $N = 1000$; Nie & Tatsuno, 2012). Therefore, $\theta_{12}^{(k,N)}$ could be a useful measure for estimating the sum of connection weights in electrophysiological recordings.

3.3 The IG Measures for Three- to Five-Neuron Interactions, ($\boldsymbol{\theta_{123}^{(k,10)}}$, $\boldsymbol{\theta_{1234}^{(k,10)}}$, $\boldsymbol{\theta_{12345}^{(k,10)}}$). To investigate whether the brain processes information with higher-order neural interactions, several studies have started using the IG measures with a couple of neuronal interactions (Ohiorhenuan et al., 2010; Ganmor, Segev, & Schneidman, 2011; Shimazaki et al., 2012). Therefore, it is important to understand how the IG measures at these interaction levels are influenced by correlated and background inputs. For the simplified 10-neuron network, they are calculated as

$$\theta_{123}^{(10,10)} = \log \frac{p_{111\cdot 0000000} p_{001\cdot 0000000} p_{010\cdot 0000000} p_{100\cdot 0000000}}{p_{011\cdot 0000000} p_{101\cdot 0000000} p_{110\cdot 0000000} p_{000\cdot 0000000}}, \quad (Full\ LLM) \tag{3.8}$$

$$\theta_{123}^{(k,10)} = \log \frac{p_{111\cdot \underbrace{0\ldots0}_{k-3}\cdot\underbrace{*\ldots*}_{10-k}} p_{001\cdot \underbrace{0\ldots0}_{k-3}\cdot\underbrace{*\ldots*}_{10-k}} p_{010\cdot \underbrace{0\ldots0}_{k-3}\cdot\underbrace{*\ldots*}_{10-k}} p_{100\cdot \underbrace{0\ldots0}_{k-3}\cdot\underbrace{*\ldots*}_{10-k}}}{p_{011\cdot \underbrace{0\ldots0}_{k-3}\cdot\underbrace{*\ldots*}_{10-k}} p_{101\cdot \underbrace{0\ldots0}_{k-3}\cdot\underbrace{*\ldots*}_{10-k}} p_{110\cdot \underbrace{0\ldots0}_{k-3}\cdot\underbrace{*\ldots*}_{10-k}} p_{000\cdot \underbrace{0\ldots0}_{k-3}\cdot\underbrace{*\ldots*}_{10-k}}}, \tag{3.9}$$

$$(Partial\ LLM)$$

$$\theta_{1234}^{(10,10)} = \log \frac{p_{1111\cdot 000000} \cdot p_{0011\cdot 000000} \cdot p_{0000\cdot 000000}^{\binom{4}{2}}}{p_{0111\cdot 000000}^{\binom{4}{1}} \cdot p_{0001\cdot 000000}^{\binom{4}{1}}}, \quad (Full\ LLM) \tag{3.10}$$

$$\theta_{1234}^{(k,10)} = \log \frac{p_{1111\cdot \underbrace{0\ldots0}_{k-4}\cdot\underbrace{*\ldots*}_{10-k}} \cdot p_{0011\cdot \underbrace{0\ldots0}_{k-4}\cdot\underbrace{*\ldots*}_{10-k}}^{\binom{4}{2}} \cdot p_{0000\cdot \underbrace{0\ldots0}_{k-4}\cdot\underbrace{*\ldots*}_{10-k}}}{p_{0111\cdot \underbrace{0\ldots0}_{k-4}\cdot\underbrace{*\ldots*}_{10-k}}^{\binom{4}{1}} \cdot p_{0001\cdot \underbrace{0\ldots0}_{k-4}\cdot\underbrace{*\ldots*}_{10-k}}^{\binom{4}{1}}},$$

$$(Partial\ LLM) \tag{3.11}$$

$$\theta_{12345}^{(10,10)} = \log \frac{p_{11111\cdot 00000} \cdot p_{00111\cdot 00000}^{\binom{5}{2}} \cdot p_{00001\cdot 00000}^{\binom{5}{1}}}{p_{01111\cdot 00000}^{\binom{5}{1}} \cdot p_{00011\cdot 00000}^{\binom{5}{2}} \cdot p_{00000\cdot 00000}},$$

$$(Full\ LLM) \tag{3.12}$$

$$\theta_{12345}^{(k,10)} = \log \frac{p_{11111\cdot \underbrace{0\ldots0}_{k-5}\cdot\underbrace{*\ldots*}_{10-k}} \cdot p_{00111\cdot \underbrace{0\ldots0}_{k-5}\cdot\underbrace{*\ldots*}_{10-k}}^{\binom{5}{2}} \cdot p_{00001\cdot \underbrace{0\ldots0}_{k-5}\cdot\underbrace{*\ldots*}_{10-k}}^{\binom{5}{1}}}{p_{01111\cdot \underbrace{0\ldots0}_{k-5}\cdot\underbrace{*\ldots*}_{10-k}}^{\binom{5}{1}} \cdot p_{00011\cdot \underbrace{0\ldots0}_{k-5}\cdot\underbrace{*\ldots*}_{10-k}}^{\binom{5}{2}} \cdot p_{00000\cdot \underbrace{0\ldots0}_{k-5}\cdot\underbrace{*\ldots*}_{10-k}}}.$$

$$(Partial\ LLM) \tag{3.13}$$

Note that $\binom{m}{i}$ represents a binomial coefficient and that $p_{x_1\ldots x_m \cdot x_{m+1}\ldots x_{10}}^{\binom{m}{i}}$ runs over the possible combinations on the first m variables.

The analytical results for $\theta_{123}^{(k,10)}$, $\theta_{1234}^{(k,10)}$, and $\theta_{12345}^{(k,10)}$ are plotted from Figures 2E to 2J. When a correlated input W is 0, all the measures are zero regardless of the existence of a background input h (see Figures 2E, 2G, and 2I). Since the network reduces to a Hopfield-type network where $W = 0$, the result is consistent with the finding that the energy function has terms only up to the second order. For $W > 0$, the IG measures deviate from 0 because a nonzero W introduces higher-order interactions. The analytical calculation shows that $\theta_{123}^{(k,10)}$ is affected monotonically by W (see Figure 2E) while $\theta_{1234}^{(k,10)}$ and $\theta_{12345}^{(k,10)}$ are influenced in a nonlinear manner (see Figures 2G and 2I). Interestingly, $\theta_{123}^{(k,10)}$ was less affected by W if there was a background input h (data not shown), as was the case for the pairwise IG measure $\theta_{12}^{(k,10)}$. This tendency was not obvious for the other IG measures $\theta_{1234}^{(k,10)}$ and $\theta_{12345}^{(k,10)}$. For all the IG measures investigated here, the values approach zero when the order of LLM k increases. When a background input h is varied, the IG measures stay very close to 0 if there is no correlated input W (see Figures 2F, 2H, and 2J). However, when $W > 0$, the IG measures are more

strongly influenced (data not shown). The range of modulation for $W > 0$ was approximately on the order of 0.1, almost 10 to 10^3 times larger than when $W = 0$. The values approach zero when the order of LLM k increases, suggesting that the IG measures calculated by higher-order LLM may be more robust to interferences from a background input h.

In summary, the analysis shows that the IG measures for three- to five-neuron interactions are affected by a correlated input W in a highly nonlinear manner. The influence by a background input h was insignificantly small if the correlated input did not exist, but it increased significantly when the correlated input was present.

3.4 The IG Measures for Six- to Ten-Neuron Interactions, ($\theta^{(k,10)}_{123456}$, $\theta^{(k,10)}_{1234567}$, $\theta^{(k,10)}_{12345678}$, $\theta^{(k,10)}_{123456789}$, $\theta^{(10,10)}_{12345678910}$). The IG measures with this many neuronal interactions have not yet been used in data analysis. However, recent developments in recording technology should allow the simultaneous recording of a large number of neurons in the near future. Therefore, it is important to investigate how these IG measures are influenced by correlated and background inputs. They are calculated as follows:

$$\theta^{(10,10)}_{123456} = \log \frac{p_{111111\cdot 0000} \cdot p_{001111\cdot 0000}^{\binom{6}{2}} \cdot p_{000011\cdot 0000}^{\binom{6}{2}} \cdot p_{000000\cdot 0000}}{p_{011111\cdot 0000}^{\binom{6}{1}} \cdot p_{000111\cdot 0000}^{\binom{6}{3}} \cdot p_{000001\cdot 0000}^{\binom{6}{1}}}, \quad (Full\ LLM) \tag{3.14}$$

$$\theta^{(k,10)}_{123456} = \log \left(\frac{p_{111111\cdot \underbrace{0\ldots0}_{k-6} \cdot \underbrace{*\ldots*}_{10-k}} \cdot p_{001111\cdot \underbrace{0\ldots0}_{k-6} \cdot \underbrace{*\ldots*}_{10-k}}^{\binom{6}{2}}}{p_{011111\cdot \underbrace{0\ldots0}_{k-6} \cdot \underbrace{*\ldots*}_{10-k}}^{\binom{6}{1}} \cdot p_{000111\cdot \underbrace{0\ldots0}_{k-6} \cdot \underbrace{*\ldots*}_{10-k}}^{\binom{6}{3}}} \times \frac{p_{000011\cdot \underbrace{0\ldots0}_{k-6} \cdot \underbrace{*\ldots*}_{10-k}}^{\binom{6}{2}} \cdot p_{000000\cdot \underbrace{0\ldots0}_{k-6} \cdot \underbrace{*\ldots*}_{10-k}}}{p_{000001\cdot \underbrace{0\ldots0}_{k-6} \cdot \underbrace{*\ldots*}_{10-k}}^{\binom{6}{1}}} \right). \quad (Partial\ LLM) \tag{3.15}$$

$$\theta^{(10,10)}_{1234567} = \log \left(\frac{p_{1111111\cdot 000} \cdot p_{0011111\cdot 000}^{\binom{7}{2}}}{p_{0111111\cdot 000}^{\binom{7}{1}} \cdot p_{0001111\cdot 000}^{\binom{7}{3}}} \times \frac{p_{0000111\cdot 000}^{\binom{7}{3}} \cdot p_{0000001\cdot 000}^{\binom{7}{1}}}{p_{0000011\cdot 000}^{\binom{7}{2}} \cdot p_{0000000\cdot 000}} \right), \quad (Full\ LLM) \tag{3.16}$$

$$\theta^{(k,10)}_{1234567} = \log\left(\frac{p_{1111111\cdot\underbrace{0\ldots0}_{k-7}\cdot\underbrace{*\ldots*}_{10-k}} \cdot p_{0011111\cdot\underbrace{0\ldots0}_{k-7}\cdot\underbrace{*\ldots*}_{10-k}}^{\binom{7}{2}}}{p_{0111111\cdot\underbrace{0\ldots0}_{k-7}\cdot\underbrace{*\ldots*}_{10-k}}^{\binom{7}{1}} \cdot p_{0001111\cdot\underbrace{0\ldots0}_{k-7}\cdot\underbrace{*\ldots*}_{10-k}}^{\binom{7}{3}}} \times \frac{p_{0000111\cdot\underbrace{0\ldots0}_{k-7}\cdot\underbrace{*\ldots*}_{10-k}}^{\binom{7}{3}} \cdot p_{0000001\cdot\underbrace{0\ldots0}_{k-7}\cdot\underbrace{*\ldots*}_{10-k}}^{\binom{7}{1}}}{p_{0000011\cdot\underbrace{0\ldots0}_{k-7}\cdot\underbrace{*\ldots*}_{10-k}}^{\binom{7}{2}} \cdot p_{0000000\cdot\underbrace{0\ldots0}_{k-7}\cdot\underbrace{*\ldots*}_{10-k}}} \right), \quad (Partial\ LLM) \tag{3.17}$$

$$\theta^{(10,10)}_{12345678} = \log\left(\frac{p_{11111111\cdot00} \cdot p_{00111111\cdot00}^{\binom{8}{2}} \cdot p_{00001111\cdot00}^{\binom{8}{4}}}{p_{01111111\cdot00}^{\binom{8}{1}} \cdot p_{00011111\cdot00}^{\binom{8}{3}}} \times \frac{p_{00000011\cdot00}^{\binom{8}{2}} \cdot p_{00000000\cdot00}}{p_{00000111\cdot00}^{\binom{8}{3}} \cdot p_{00000001\cdot00}^{\binom{8}{1}}} \right), \quad (Full\ LLM) \tag{3.18}$$

$$\theta^{(k,10)}_{12345678} = \log\left(\frac{p_{11111111\cdot\underbrace{0\ldots0}_{k-8}\cdot\underbrace{*\ldots*}_{10-k}} \cdot p_{00111111\cdot\underbrace{0\ldots0}_{k-8}\cdot\underbrace{*\ldots*}_{10-k}}^{\binom{8}{2}} \cdot p_{00001111\cdot\underbrace{0\ldots0}_{k-8}\cdot\underbrace{*\ldots*}_{10-k}}^{\binom{8}{4}}}{p_{01111111\cdot\underbrace{0\ldots0}_{k-8}\cdot\underbrace{*\ldots*}_{10-k}}^{\binom{8}{1}} \cdot p_{00011111\cdot\underbrace{0\ldots0}_{k-8}\cdot\underbrace{*\ldots*}_{10-k}}^{\binom{8}{3}}} \times \frac{p_{00000011\cdot\underbrace{0\ldots0}_{k-8}\cdot\underbrace{*\ldots*}_{10-k}}^{\binom{8}{2}} \cdot p_{00000000\cdot\underbrace{0\ldots0}_{k-8}\cdot\underbrace{*\ldots*}_{10-k}}}{p_{00000111\cdot\underbrace{0\ldots0}_{k-8}\cdot\underbrace{*\ldots*}_{10-k}}^{\binom{8}{3}} \cdot p_{00000001\cdot\underbrace{0\ldots0}_{k-8}\cdot\underbrace{*\ldots*}_{10-k}}^{\binom{8}{1}}} \right), \quad (Partial\ LLM) \tag{3.19}$$

$$\theta^{(10,10)}_{123456789} = \log\left(\frac{p_{111111111\cdot0} \cdot p_{001111111\cdot0}^{\binom{9}{2}} \cdot p_{000011111\cdot0}^{\binom{9}{4}}}{p_{011111111\cdot0}^{\binom{9}{1}} \cdot p_{000111111\cdot0}^{\binom{9}{3}} \cdot p_{000001111\cdot0}^{\binom{9}{4}}} \times \frac{p_{000000111\cdot0}^{\binom{9}{3}} \cdot p_{000000001\cdot0}^{\binom{9}{1}}}{p_{000000011\cdot0}^{\binom{9}{2}} \cdot p_{000000000\cdot0}} \right), \quad (Full\ LLM) \tag{3.20}$$

$$\theta^{(9,10)}_{123456789} = \log\left(\frac{p_{111111111\cdot *} \cdot p_{001111111\cdot *}^{\binom{9}{2}} \cdot p_{000011111\cdot *}^{\binom{9}{4}}}{p_{011111111\cdot *}^{\binom{9}{1}} \cdot p_{000111111\cdot *}^{\binom{9}{3}} \cdot p_{000001111\cdot *}^{\binom{9}{4}}} \times \frac{p_{000000111\cdot *}^{\binom{9}{3}} \cdot p_{000000001\cdot *}^{\binom{9}{1}}}{p_{000000011\cdot *}^{\binom{9}{2}} \cdot p_{000000000\cdot *}} \right), \quad (Partial\ LLM) \tag{3.21}$$

$$\theta^{(10,10)}_{12345678910} = \log\left(\frac{p_{1111111111} \cdot p_{0011111111}^{\binom{10}{2}} \cdot p_{0000111111}^{\binom{10}{4}}}{p_{0111111111}^{\binom{10}{1}} \cdot p_{0001111111}^{\binom{10}{3}} \cdot p_{0000011111}^{\binom{10}{5}}} \times \frac{p_{0000001111}^{\binom{10}{4}} \cdot p_{0000000011}^{\binom{10}{2}} \cdot p_{0000000000}}{p_{0000000111}^{\binom{10}{3}} \cdot p_{0000000001}^{\binom{10}{1}}} \right), \quad (Full\ LLM) \tag{3.22}$$

Note that the IG measure for a 9-neuron interaction $\theta^{(k,10)}_{123456789}$ has only one partially expanded LLM ($k = 9$) and the IG measure for a 10-neuron interaction $\theta^{(10,10)}_{12345678910}$ has the full LLM ($k = 10$) only.

The analytical results for $\theta^{(k,10)}_{123456}$, $\theta^{(k,10)}_{1234567}$, $\theta^{(k,10)}_{12345678}$, $\theta^{(k,10)}_{123456789}$, and $\theta^{(10,10)}_{12345678910}$ are shown in Figure 3. The general trend of dependency of these measures on correlated and background inputs was similar to that of $\theta^{(k,10)}_{1234}$ and $\theta^{(k,10)}_{12345}$. When $W = 0$, all the measures are zero regardless of the existence of a background input h (see Figures 3A, 3C, 3E, 3G, and 3I). However, when $W > 0$, especially when $W > 0.5\ (= 5J)$, the IG measures deviated from zero in a highly nonlinear manner. The values tended to approach zero when the order of LLM k increased, although the trend was less obvious as compared to IG measures involving three to seven neurons. When a background input h is varied, the IG measures stay very close to zero if there is no correlated input W (see Figures 3B, 3D, 3F, 3H, and 3J). When $W > 0$, the IG measures are more strongly influenced (data not shown). The range of modulation was almost 10^3- to 10^5-fold larger than when $W = 0$. When the order of LLM k increased, the values became less variable.

In summary, this analysis shows that the IG measures for 6- to 10-neuron interactions are affected by a correlated input W in a highly nonlinear manner. The influence by a background input h was insignificantly small if $W = 0$ but increased significantly for $W > 0$.

4 Simulation Study of IG Measures with Asymmetric Connections

Although the analytical relationship between the IG measures and network parameters is useful, we had to apply a strong constraint of uniform connectivity between neurons. We also had to use a small network size of

10 neurons to obtain the analytical solutions. These constraints made it difficult to obtain further insights into a more general situation such as with asymmetric connections. Therefore, we extended our investigation using numerical computer simulation.

First, to demonstrate the accuracy of the simulation, we numerically calculated the IG measures for a uniformly connected 10-neuron network and compared them with the analytical results obtained in the previous section. Second, we extended the connections from uniform to asymmetric. We investigated how external inputs (correlated input W and background input h) influenced the IG measures and how the network size affected their relationship with network parameters. In addition, we investigated how the magnitude of the asymmetry of connection weights influenced the IG measures.

4.1 Comparison Between Computer Simulations and Analytical Results. We performed numerical simulations using ten uniformly connected Ginzburg and Sompolinsky (1994) neurons. We computed the IG measures from 1-neuron interaction ($\theta_1^{(k,10)}$) to 10-neuron interactions ($\theta_{12345678910}^{(10,10)}$) with all possible LLM orders k, corresponding to Figures 2 and 3. We calculated the IG measures by sampling a correlated input W from 0 to $50J$ with an increment of $5J$. We also calculated the IG measures by sampling a background input h from 0 to $5J$ with an increment of $0.5J$. At each value of W and h, we performed 100 simulation trials where each trial consisted of 10^6 updates. The parameter m that controls the firing probability of a model neuron in equation 2.24 was set to 1. The results are reported as the mean $\pm$ SEM.

Figure 4 shows the representative examples in which we compare the values of numerical simulations and the corresponding analytical results. For clarity, we showed the results only for the single IG measure $\theta_1^{(k,10)}$ (see Figures 4A and 4B), the pairwise IG measure $\theta_{12}^{(k,10)}$ (see Figures 4C and 4D), the 9-neuron IG measure $\theta_{123456789}^{(k,10)}$ (see Figures 4E and 4F), and the 10-neuron IG measure $\theta_{12345678910}^{(10,10)}$ (see Figures 4G and 4H). We also plotted the results only for the lowest and highest LLM orders $\theta_1^{(1,10)}$; and $\theta_1^{(10,10)}$ for the single IG measure (see Figures 4A and 4B), $\theta_{12}^{(2,10)}$ and $\theta_{12}^{(10,10)}$ for the pairwise IG measure (see Figures 4C and 4D), $\theta_{123456789}^{(9,10)}$ and $\theta_{123456789}^{(10,10)}$ for the 9-neuron IG measure (Figures 4E and 4F), and $\theta_{12345678910}^{(10,10)}$ for the 10-neuron IG measure (see Figures 4G and 4H). Figure 4 shows that the numerical simulations and analytical results strongly agree; all analytical results are included within the mean $\pm$ SEM of the values obtained with the numerical simulations. We also confirmed that the same relationship holds true for all the IG measures that were not included in Figure 4 and for all possible LLM orders. Taken together, these results demonstrate that the numerical simulation reproduces the analytical results accurately and

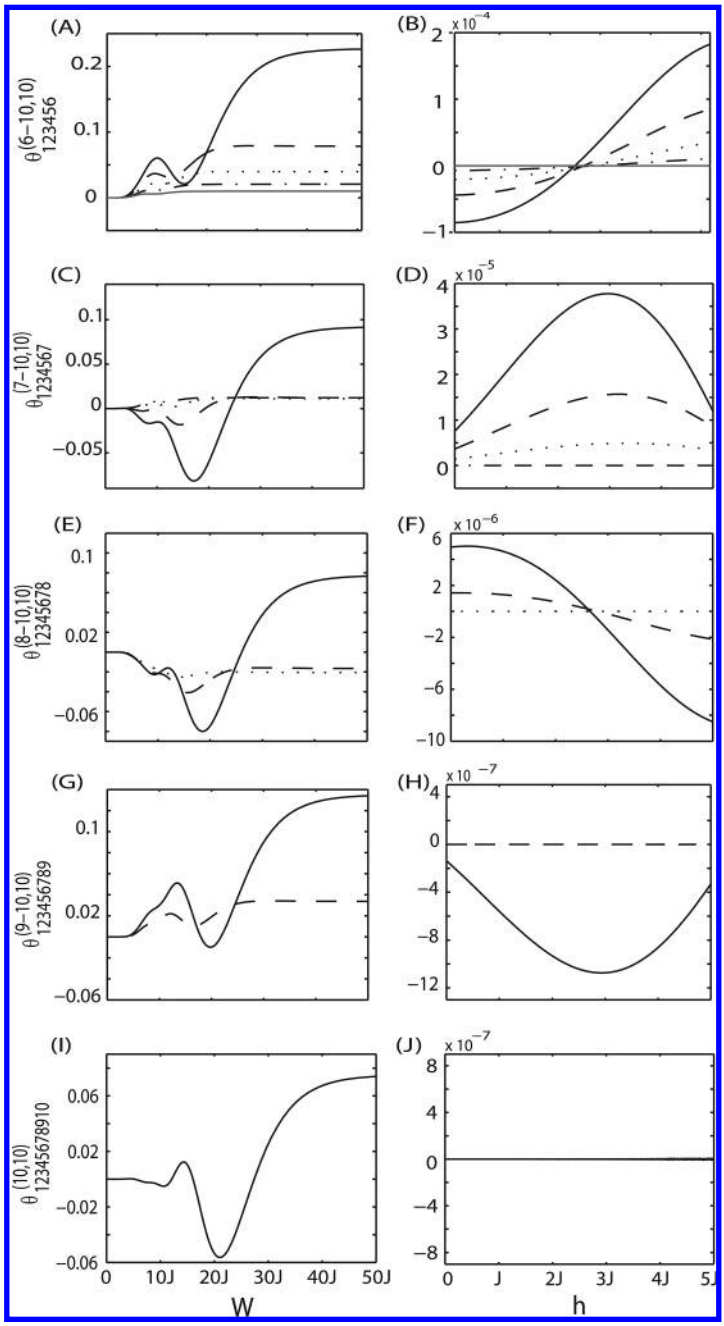
(A)
(B)
(C)
(D)
(E)
(F)
(G)
(H)
(I)
(J)
θ(6−10,10) 123456
θ(7−10,10) 1234567
θ(8−10,10) 12345678
θ(9−10,10) 123456789
θ(10,10) 12345678910
x 10^−4
x 10^−5
x 10^−6
x 10^−7
0 10J 20J 30J 40J 50J
W
0 J 2J 3J 4J 5J
h

that they could be used for investigating the relationship between the IG measures and network parameters in more general settings such as with asymmetric connections.

4.2 Relationship Between the IG Measures and External Inputs for Asymmetrically Connected Networks. In this section, we extended a uniformly connected neural network to an asymmetrically connected one. We numerically calculated the IG measures for up to 10-neuronal interactions with $N = 10$ and 1000 neurons. Asymmetric connections were set as $J_{ij} = 1/N + \varepsilon_{ij}$ at each simulation trial, where ε_{ij} was a random number drawn from the normal distribution $\mathrm{N}(m, \sigma^2)$ with the mean $m = 0$ and variance $\sigma^2 = 1/N$, respectively. Without losing generality, we calculated the IG measures for a specific neuron group as follows. For the pairwise IG measure $\theta_{12}^{(k,N)}$, we selected neurons 1 and 2 and set their connection weights to $J_{12} = 1/N + \varepsilon_{12}$ and $J_{21} = \frac{2}{N} - J_{12}$. In this way, the magnitude of their total connections was kept constant ($J_{12} + J_{21} = 2/N$). We applied this

Figure 3: Relationship between the IG measures ($\theta_{123456}^{(k,10)}$, $\theta_{1234567}^{(k,10)}$, $\theta_{12345678}^{(k,10)}$, $\theta_{123456789}^{(k,10)}$, $\theta_{12345678910}^{(10,10)}$), a correlated input ($W$), and a background input (h) for a 10-neuron uniformly connected network. The network parameters are set as$J = 1/10$ and $h_0 = 0.5$. W is modified in the range of $[0, 50J]$ and h is modified in the range of $[0, 5J]$. (A) $\theta_{123456}^{(k,10)}$ when a correlated input (W) is varied in the absence of a background input ($h = 0$). (B) $\theta_{123456}^{(k,10)}$ when background input (h) is varied in the absence of a correlated input ($W = 0$). $\theta_{123456}^{(6,10)}$, $\theta_{123456}^{(7,10)}$, $\theta_{123456}^{(8,10)}$, $\theta_{123456}^{(9,10)}$, and $\theta_{123456}^{(10,10)}$ are represented by a black solid line, a black dashed line, a black dotted line, a black dash-dot line, and a gray solid line. (C) $\theta_{1234567}^{(k,10)}$ when a correlated input (W) is varied in the absence of a background input ($h = 0$). (D) $\theta_{1234567}^{(k,10)}$ when a background input (h) is varied in the absence of a correlated input ($W = 0$). $\theta_{1234567}^{(7,10)}$, $\theta_{1234567}^{(8,10)}$, $\theta_{1234567}^{(9,10)}$, and $\theta_{1234567}^{(10,10)}$ are represented by a black solid line, a black dashed line, a black dotted line, and a black dash-dot line. (E) $\theta_{12345678}^{(k,10)}$ when a correlated input (W) is varied in the absence of a background input ($h = 0$). (F) $\theta_{12345678}^{(k,10)}$ when a background input (h) is varied in the absence of a correlated input ($W = 0$). $\theta_{12345678}^{(8,10)}$, $\theta_{12345678}^{(9,10)}$, and $\theta_{12345678}^{(10,10)}$ are represented by a black solid line, a black dashed line, and a black dotted line. (G) $\theta_{123456789}^{(k,10)}$ when a correlated input (W) is varied in the absence of a background input ($h = 0$). (H) $\theta_{123456789}^{(k,10)}$ when a background input (h) is varied in the absence of a correlated input ($W = 0$). $\theta_{123456789}^{(9,10)}$ and $\theta_{123456789}^{(10,10)}$ are represented by a black solid line and a black dashed line. (I) $\theta_{12345678910}^{(10,10)}$ when a correlated input (W) is varied in the absence of a background input ($h = 0$). (J) $\theta_{12345678910}^{(10,10)}$ when a background input (h) is varied in the absence of a correlated input ($W = 0$). $\theta_{12345678910}^{(10,10)}$ is represented by a black solid line.

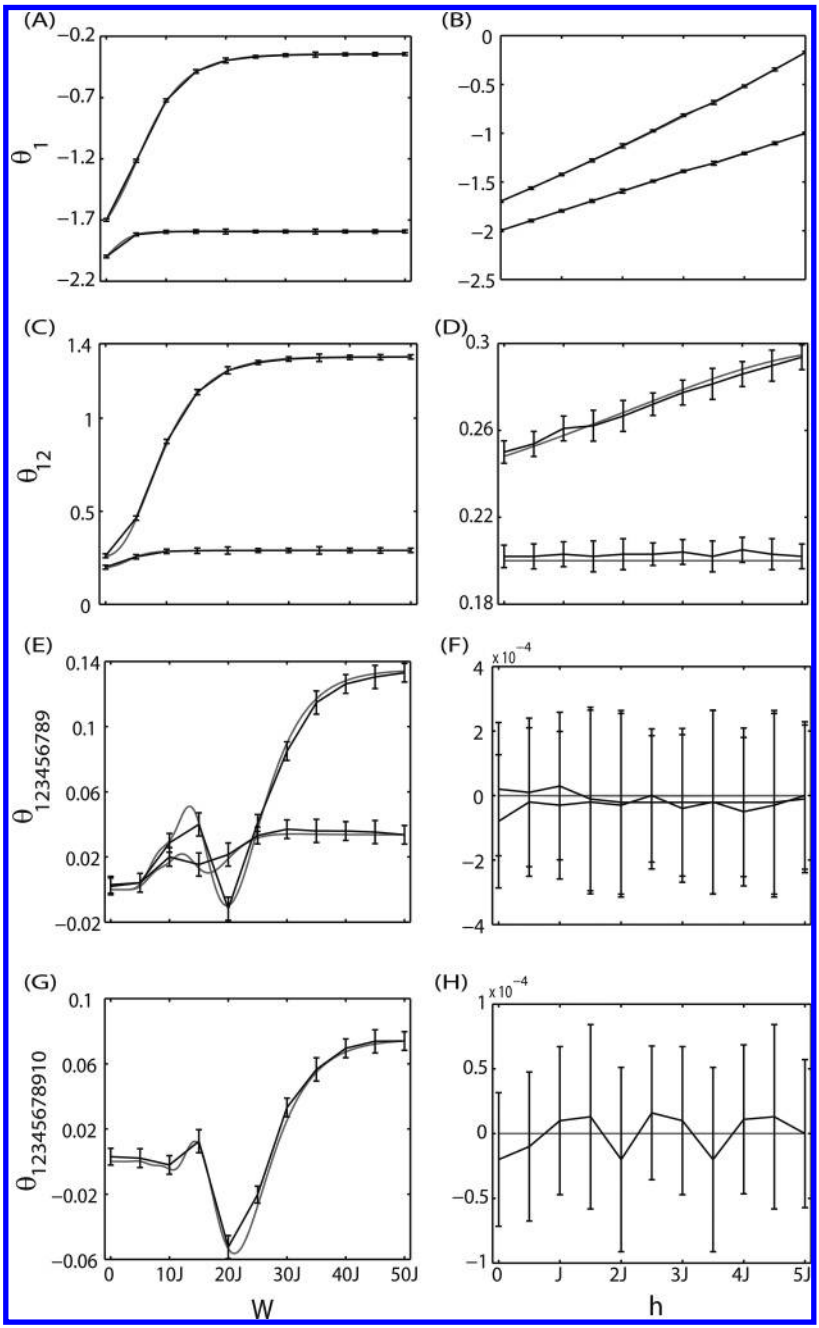
(A)
(B)
(C)
(D)
(E)
(F)
(G)
(H)
θ1
θ12
θ123456789
θ12345678910
x 10−4
W
h

constraint because we wanted to assess the robustness of the relationship $\theta_{12}^{(k,N)} \sim (J_{12} + J_{21})$. The other connections were set following $J_{ij} = 1/N + \varepsilon_{ij}$. Similarly, for the three-neuron IG measure $\theta_{123}^{(k,N)}$, we selected the neurons 1, 2, and 3 and set their connection weights to ($J_{12} = 1/N + \varepsilon_{12}$ and $J_{21} = 2/\mathrm{N} - J_{12}$), ($J_{23} = 1/N + \varepsilon_{23}$ and $J_{32} = 2/N - J_{32}$), and ($J_{31} = 1/N + \varepsilon_{31}$ and $J_{13} = 2/\mathrm{N} - J_{31}$). For clarity of the analysis, these constraints were applied to investigate the robustness of $\theta_{123}^{(k,N)}$. The other connections were set following $J_{ij} = 1/N + \varepsilon_{ij}$. We used the same procedure for all the other IG measures with four or more neuronal interactions. The influence of a common input W was investigated in the range of $[0, 50J]$. Similarly, the influence of a background input $h_i = h$ was investigated at 0 and $5J$. As the theoretical calculation and simulation for uniform connections showed that the IG measures were influenced by the common input W strongly (see Figures 2 to 4), more data points were sampled for W. Each simulation trial consisted of 10^6 updates, and 100 trials were performed at each W and h value. The parameter m that controls the firing probability of a model neuron in equation 2.24 was set to 1. The results are presented as the mean ± SEM.

4.2.1 The IG Measures for Single and Pairwise Interactions, ($\theta_1^{(k,N)}$, $\theta_{12}^{(k,N)}$). Figures 5A and 5B show how the single IG measure $\theta_1^{(k,10)}$ is influenced by a

Figure 4: Comparison between a numerical simulation and an analytical solution. The results of 100 simulation trials (mean ± SEM) are plotted against the theoretical calculation in Figures 2 and 3. The network parameters are set as $J = 1/10$ and $h_0 = 0.5$. W is modified in the range of $[0, 50J]$, and h is modified in the range of $[0, 5J]$. The numerical simulations are represented by solid lines with error bars. The analytical solutions are represented by gray lines. (A) Comparison for the single IG measures $\theta_1^{(1,10)}$ and $\theta_1^{(10,10)}$ when correlated input (W) is varied in the absence of a background input ($h = 0$). (B) Comparison for the single IG measures $\theta_1^{(1,10)}$ and $\theta_1^{(10,10)}$ when background input (h) is varied in the absence of a correlated input ($W = 0$). (C) Comparison for the pairwise IG measures $\theta_{12}^{(1,10)}$ and $\theta_{12}^{(10,10)}$ when correlated input (W) is varied in the absence of a background input ($h = 0$). (D) Comparison for the pairwise IG measures $\theta_{12}^{(1,10)}$ and $\theta_{12}^{(10,10)}$ when background input (h) is varied in the absence of a correlated input ($W = 0$). (E) Comparison for the 9-neuron IG measures $\theta_{123456789}^{(1,10)}$ and $\theta_{123456789}^{(10,10)}$ when correlated input (W) is varied in the absence of a background input ($h = 0$). (F) Comparison for the 9-neuron IG measures $\theta_{123456789}^{(1,10)}$ and $\theta_{123456789}^{(10,10)}$ when background input (h) is varied in the absence of a correlated input ($W = 0$). (G) Comparison for the 10-neuron IG measures $\theta_{12345678910}^{(1,10)}$ and $\theta_{12345678910}^{(10,10)}$ when correlated input (W) is varied in the absence of a background input ($h = 0$). (H) Comparison for the 10-neuron IG measures $\theta_{12345678910}^{(1,10)}$ and $\theta_{12345678910}^{(10,10)}$ when background input (h) is varied in the absence of a correlated input ($W = 0$).

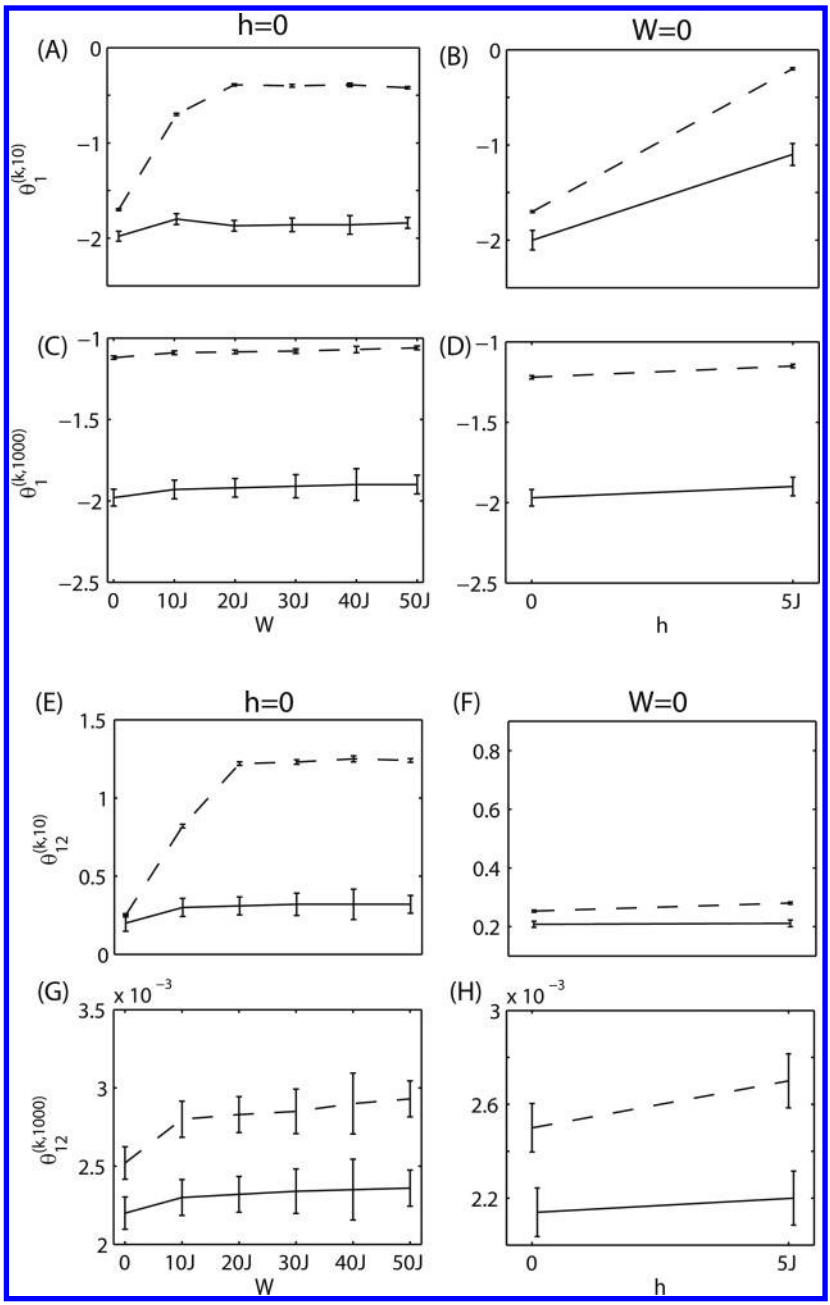
h=0
W=0
(A)
(B)
(C)
(D)
(E)
(F)
(G)
(H)
$\theta_1^{(k,10)}$
$\theta_1^{(k,1000)}$
$\theta_{12}^{(k,10)}$
$\theta_{12}^{(k,1000)}$
x 10^-3
0 10J 20J 30J 40J 50J
W
0 5J
h

common input W and a background input h, for an asymmetric network of 10 neurons. For clarity, we showed the results for the lowest and highest LLM orders only ($k = 1$, dashed line; and $k = 10$, solid line), but we confirmed that the IG measures with $k = 2$ to $k = 9$ reside between $k = 1$ and $k = 10$. The simulation showed that $\theta_1^{(1,10)}$ (dashed line, lowest LLM order) was affected by both the common input and the background input. However, $\theta_1^{(10,10)}$ (solid line, highest LLM order) was robust against the common input and was related to the background input only. Note the similarity between the simulation results in Figure 5 and the analytical results for a uniformly connected network in Figure 2. When the size of the network was increased to $N = 1000$, the influence of a common input became significantly smaller (see Figure 5C), even for $\theta_1^{(1,1000)}$ (dashed line, lowest LLM order). Note that the values of $\theta_1^{(10,10)}$ and $\theta_1^{(10,1000)}$ were more consistent than those of $\theta_1^{(1,10)}$ and $\theta_1^{(1,1000)}$, although their network size was 100 times different (see Figures 5A–5D). Furthermore, we confirmed that the values of $\theta_1^{(10,10)}$ and $\theta_1^{(10,1000)}$ were close to the values predicted from equation 3.1, even under the influence of both the common input and the background input (data not shown). This result suggests that $\theta_1^{(1,10)}$ and $\theta_1^{(10,1000)}$, the single IG measure

Figure 5: Relationship between the IG measures ($\theta_1^{(k,N)}$, $\theta_{12}^{(k,N)}$), a correlated input (W), and a background input (h) for an asymmetrically connected network. For a 10-neuron network ($N = 10$), the network parameters are set as $J = 1/10$ and $h_0 = 0.5$. For a 1000-neuron network ($N = 1000$), the network parameters are set as $J = 1/1000$ and $h_0 = 0.005$. W is sampled from 0 to $50J$, and h is sampled at 0 and $5J$. The IG measures with the lowest LLM order (e.g., $\theta_1^{(1,10)}$) are represented by a dashed line. The IG measures with the highest LLM order (e.g., $\theta_1^{(10,10)}$) are represented by a solid line. (A) The single IG measures for a 10-neuron network $\theta_1^{(1,10)}$ and $\theta_1^{(10,10)}$ when a correlated input (W) is varied in the absence of a background input ($h = 0$). (B) The single IG measures for a 10-neuron network $\theta_1^{(1,10)}$ and $\theta_1^{(10,10)}$ when background input (h) is varied in the absence of a correlated input ($W = 0$). (C) The single IG measures for a 1000-neuron network $\theta_1^{(1,1000)}$ and $\theta_1^{(10,1000)}$ when a correlated input (W) is varied in the absence of a background input ($h = 0$). (D) The single IG measures for a 1000-neuron network $\theta_1^{(1,1000)}$ and $\theta_1^{(10,1000)}$ when background input (h) is varied in the absence of a correlated input ($W = 0$). (E) The pairwise IG measures for a 10-neuron network $\theta_{12}^{(2,10)}$ and $\theta_{12}^{(10,10)}$ when a correlated input (W) is varied in the absence of a background input ($h = 0$). (F) The pairwise IG measures for a 10-neuron network $\theta_{12}^{(2,10)}$ and $\theta_{12}^{(10,10)}$ when background input (h) is varied in the absence of a correlated input ($W = 0$). (G) The pairwise IG measures for a 1000-neuron network $\theta_{12}^{(2,1000)}$ and $\theta_{12}^{(10,1000)}$ when a correlated input (W) is varied in the absence of a background input ($h = 0$). (H) The pairwise IG measures for a 1000-neuron network $\theta_{12}^{(2,1000)}$ and $\theta_{12}^{(10,1000)}$ when background input (h) is varied in the absence of a correlated input ($W = 0$).

with the highest LLM order in this study, was able to detect the background input correctly even under the influence of the common input.

For the pairwise IG measure $\theta_{12}^{(k,N)}$, the results for an asymmetric network of 10 neurons are shown in Figures 5E and 5F. The desired property of the pairwise IG measure is to detect the two-neuron interaction correctly: $\theta_{12} \sim J_{12} + J_{21} = 0.2$ for $N = 10$. We observed that $\theta_{12}^{(2,10)}$ (the measure with the lowest LLM order) was strongly influenced by a common input (see Figure 5E, dashed line), but the influence of a background input was much weaker (see Figure 5F, dashed line). In contrast, the influence of external inputs to $\theta_{12}^{(10,10)}$ (the measure with the highest LLM order) was much weaker, and $\theta_{12}^{(10,10)}$ was able to estimate the connection weight almost correctly (see Figures 5E and 5F, solid lines). It is also important to note the similarity of $\theta_{12}^{(k,10)}$ values to the corresponding analytical results for a uniform connection (see Figures 2C and 2D). When the size of the network was increased to $N = 1000$, we observed a similar tendency (see Figures 5G and 5H); $\theta_{12}^{(10,1000)}$ (solid line) was more robust against the external inputs than $\theta_{12}^{(2,1000)}$ (dashed line). Also note that $\theta_{12}^{(10,1000)}$ estimated the connection weight almost correctly: $\theta_{12}^{(10,1000)} \sim J_{12} + J_{21} = 2 \times 10^{-3}$.

In summary, the numerical simulation demonstrated that the single IG measure $\theta_1^{(10,N)}$ and the pairwise IG measure $\theta_{12}^{(10,N)}$ (highest LLM order) were able to detect the background input and the sum of connection weights, for an asymmetrically connected network. We also found that the influence of external inputs became less significant for a larger network.

4.2.2 The IG Measures for Three- to Ten-Neuron Interactions, ($\theta_{123}^{(k,N)}$, $\theta_{1234}^{(k,N)}$, $\theta_{12345}^{(k,N)}$, $\theta_{123456}^{(k,N)}$, $\theta_{1234567}^{(k,N)}$, $\theta_{12345678}^{(k,N)}$, $\theta_{123456789}^{(k,N)}$, $\theta_{12345678910}^{(k,N)}$). The influence of external inputs to the IG measures with intermediate neural interactional levels, $\theta_{123}^{(k,N)}$, $\theta_{1234}^{(k,N)}$, $\theta_{12345}^{(k,N)}$, $\theta_{123456}^{(k,N)}$, is summarized in Figure 6 and that with many neural interactional levels, $\theta_{1234567}^{(k,N)}$, $\theta_{12345678}^{(k,N)}$, $\theta_{123456789}^{(k,N)}$, $\theta_{12345678910}^{(k,N)}$, is summarized in Figure 7.

For the 3-neuron IG measure $\theta_{123}^{(k,10)}$ with a 10-neuron network, $\theta_{123}^{(3,10)}$ (the lowest LLM order) was strongly influenced by the common input (see Figure 6A, dashed line) but the influence of the background input was much weaker (see Figure 6B, dashed line). $\theta_{123}^{(10,10)}$ (the highest LLM order) was more robust for both common and background inputs (see Figures 6A and 6B, solid lines). Also, the $\theta_{123}^{(k,10)}$ values are similar to the corresponding analytical values in Figures 2E and 2F. When the size of the network was increased to $N = 1000$, the influence of external inputs on $\theta_{123}^{(k,1000)}$ almost disappeared and the values of $\theta_{123}^{(k,1000)}$ stayed around zero (see Figures 6C and 6D). This result suggests that the 3-neuron IG measure $\theta_{123}^{(k,N)}$ for an asymmetrically connected network is robust against external inputs and

that its value is likely to be found around zero if the size of the network is sufficiently large.

The results for the 4-neuron IG measure $\theta_{1234}^{(k,10)}$ with a 10-neuron network are summarized in Figures 6E and 6F. $\theta_{1234}^{(4,10)}$ (the lowest LLM order) was strongly influenced by the common input (see Figure 6E, dashed line), but the influence of the background input was much weaker (see Figure 6F, dashed line). The influence of both external inputs $\theta_{1234}^{(10,10)}$ (the highest LLM order) was negligibly small (see Figures 6E and 6F, solid lines). The $\theta_{1234}^{(k,10)}$ values were similar to the corresponding analytical values in Figures 2G and 2H. When the size of the network was increased to $N = 1000$, the influence of external inputs on $\theta_{1234}^{(k,1000)}$ disappeared (see Figures 6G and 6H). These results suggest that the nonlinear relationship between $\theta_{1234}^{(k,N)}$ and the external inputs observed for a small asymmetric network is likely to disappear for a large asymmetric network.

The results for the 5-neuron IG measure $\theta_{12345}^{(k,10)}$ with a 10-neuron network are summarized in Figures 6I and 6J. We found that the results were similar to the 4-neuron IG measure $\theta_{1234}^{(k,10)}$. Mainly, $\theta_{12345}^{(5,10)}$ (the lowest LLM order) was strongly influenced by the common input (see Figure 6I, dashed line), but the influence of the background input was much weaker (see Figure 6J, dashed line). The influence of both external inputs to $\theta_{12345}^{(10,10)}$ (the highest LLM order) was negligibly small (see Figures 6I and 6J, solid lines). The $\theta_{12345}^{(k,10)}$ values were similar to the corresponding analytical values in Figures 2I and 2J. For a network of $N = 1000$, the influence of both external inputs on $\theta_{12345}^{(k,1000)}$ disappeared (see Figures 6K and 6L). These results suggest that the nonlinear relationship between $\theta_{12345,}^{(k,N)}$ and the external inputs observed for a small asymmetric network is likely to disappear for a large asymmetric network.

The results for the 6-neuron IG measure $\theta_{123456}^{(k,10)}$ with a 10-neuron network are summarized in Figures 6M and 6N and those for $\theta_{123456}^{(k,1000)}$ with a 1000-neuron network in Figures 6O and 6P. As with the other intermediate IG measures, we found that $\theta_{123456}^{(6,10)}$ (the lowest LLM order) was strongly influenced by the common input (see Figure 6M, dashed line), but the influence of the background input was much weaker (see Figure 6N, dashed line). The influence of both external inputs to $\theta_{123456}^{(10,10)}$ (highest LLM order) was negligibly small (see Figures 6M and 6N, solid lines). The $\theta_{123456}^{(k,10)}$ values were similar to the corresponding analytical values in Figures 3A and 3B. For a network $N = 1000$, the influence of both external inputs on $\theta_{123456}^{(k,1000)}$ disappeared (see Figures 6O and 6P). These results suggest that the nonlinear relationship between $\theta_{123456}^{(k,N)}$ and the external inputs observed for a small asymmetric network is likely to disappear for a large asymmetric network.

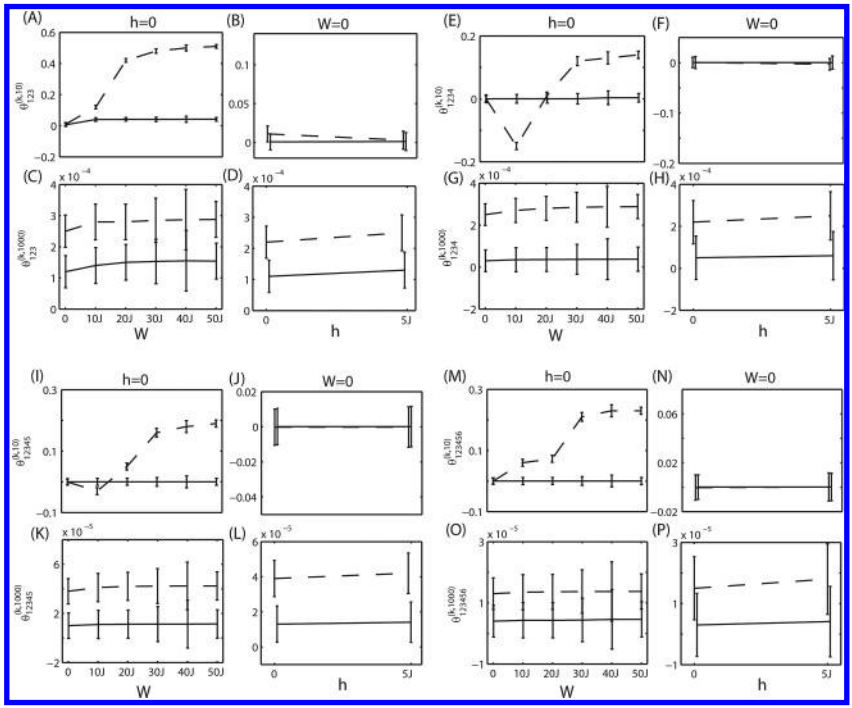

In summary, the IG measures with intermediate neural interactional levels $\theta^{(k,N)}_{123}$, $\theta^{(k,N)}_{1234}$, $\theta^{(k,N)}_{12345}$, $\theta^{(k,N)}_{123456}$, for a small asymmetrically connected network ($N = 10$) are strongly influenced by a common input. This finding was similar to the analytical solution for a uniformly connected network. However, when the size of the network becomes large (e.g., $N = 1000$), the influence by the external inputs becomes negligibly small, and these IG measures are likely to fluctuate around zero.

The influence of external inputs to the IG measures with many neural interactional levels $\theta^{(k,N)}_{1234567}$, $\theta^{(k,N)}_{12345678}$, $\theta^{(k,N)}_{123456789}$, $\theta^{(k,N)}_{12345678910}$, is summarized in Figure 7. In short, the results were very similar to those found for the IG measures with intermediate interaction levels. The IG measures with the lowest LLM orders ($\theta^{(7,10)}_{1234567}$, $\theta^{(8,10)}_{12345678}$, $\theta^{(9,10)}_{123456789}$, $\theta^{(10,10)}_{12345678910}$) were strongly influenced by a common input (see the dashed line in Figures 7A, 7E, and 7I and the solid line in Figure 7M), but the influence of a background input was negligible (see the dashed line in Figures 7A, 7E, and 7I and the solid line in Figure 7M). The influence of both external inputs to the highest-order IG measures ($\theta^{(10,10)}_{1234567}$, $\theta^{(10,10)}_{12345678}$, $\theta^{(10,10)}_{123456789}$) was negligibly small (see Figures 7A, 7B, 7E, 7F, 7I, and 7J, solid lines). When the size of a network was increased to $N = 1000$, the influence of both external inputs on the IG measures disappeared (see Figures 7C, 7D, 7G, 7H, 7K, 7L, 7O, and 7P). These results

suggest that the nonlinear relationship between the IG measures with many neuronal interactions, $\theta^{(k,N)}_{1234567}$, $\theta^{(k,N)}_{12345678}$, $\theta^{(k,N)}_{123456789}$, $\theta^{(k,N)}_{12345678910}$, and the external inputs observed for a small asymmetric network is likely to disappear for a large asymmetric network.

Figure 6: Relationship between the IG measures ($\theta^{(k,N)}_{123}$, $\theta^{(k,N)}_{1234}$, $\theta^{(k,N)}_{12345}$, $\theta^{(k,N)}_{123456}$), a correlated input (W), and a background input (h) for an asymmetrically connected network. For a 10-neuron network ($N = 10$), the network parameters are set as$J = 1/10$ and $h_0 = 0.5$. For a 1000-neuron network ($N = 1000$), the network parameters are set as $J = 1/1000$ and $h_0 = 0.005$. W is sampled from 0 to 50J, and h is sampled at 0 and 5J. The IG measures with the lowest LLM order (e.g., $\theta^{(3,10)}_{123}$) are represented by a dashed line. The IG measures with the highest LLM order (e.g., $\theta^{(10,10)}_{123}$) are represented by a solid line. (A) The 3-neuron IG measures for a 10-neuron network $\theta^{(3,10)}_{123}$ and $\theta^{(10,10)}_{123}$ when a correlated input (W) is varied in the absence of a background input ($h = 0$). (B) The 3-neuron IG measures for a 10-neuron network $\theta^{(3,10)}_{123}$ and $\theta^{(10,10)}_{123}$ when background input (h) is varied in the absence of a correlated input ($W = 0$). (C) The 3-neuron IG measures for a 1000-neuron network $\theta^{(3,1000)}_{123}$ and $\theta^{(10,1000)}_{123}$ when a correlated input (W) is varied in the absence of a background input ($h = 0$). (D) The 3-neuron IG measures for a 1000-neuron network $\theta^{(3,1000)}_{123}$ and $\theta^{(10,1000)}_{123}$ when background input (h) is varied in the absence of a correlated input ($W = 0$). (E) The 4-neuron IG measures for a 10-neuron network $\theta^{(4,10)}_{1234}$ and $\theta^{(10,10)}_{1234}$ when a correlated input (W) is varied in the absence of a background input ($h = 0$). (F) The 4-neuron IG measures for a 10-neuron network $\theta^{(4,10)}_{1234}$ and $\theta^{(10,10)}_{1234}$ when background input (h) is varied in the absence of a correlated input ($W = 0$). (G) The 4-neuron IG measures for a 1000-neuron network $\theta^{(4,1000)}_{1234}$ and $\theta^{(10,1000)}_{1234}$ when a correlated input (W) is varied in the absence of a background input ($h = 0$). (H) The 4-neuron IG measures for a 1000-neuron network $\theta^{(4,1000)}_{1234}$ and $\theta^{(10,1000)}_{1234}$ when background input (h) is varied in the absence of a correlated input ($W = 0$). (I) The 5-neuron IG measures for a 10-neuron network $\theta^{(5,10)}_{12345}$ and $\theta^{(10,10)}_{12345}$ when a correlated input (W) is varied in the absence of a background input ($h = 0$). (J) The 5-neuron IG measures for a 10-neuron network $\theta^{(5,10)}_{12345}$ and $\theta^{(10,10)}_{12345}$ when background input (h) is varied in the absence of a correlated input ($W = 0$). (K) The 5-neuron IG measures for a 1000-neuron neuron network $\theta^{(5,1000)}_{12345}$ and $\theta^{(10,1000)}_{12345}$ when a correlated input (W) is varied in the absence of a background input ($h = 0$). (L) The 5-neuron IG measures for a 1000-neuron network $\theta^{(5,1000)}_{12345}$ and $\theta^{(10,1000)}_{12345}$ when background input (h) is varied in the absence of a correlated input ($W = 0$). (M) The 6-neuron IG measures for a 10-neuron network $\theta^{(6,10)}_{123456}$ and $\theta^{(10,10)}_{123456}$ when a correlated input (W) is varied in the absence of a background input ($h = 0$). (N) The 6-neuron IG measures for a 10-neuron network $\theta^{(6,10)}_{123456}$ and $\theta^{(10,10)}_{123456}$ when background input (h) is varied in the absence of a correlated input ($W = 0$). (O) The 6-neuron IG measures for a 1000-neuron network $\theta^{(6,1000)}_{123456}$ and $\theta^{(10,1000)}_{123456}$ when a correlated input (W) is varied in the absence of a background input ($h = 0$). (P) The 6-neuron IG measures for a 1000-neuron network $\theta^{(6,1000)}_{123456}$ and $\theta^{(10,1000)}_{123456}$ when background input (h) is varied in the absence of a correlated input ($W = 0$).

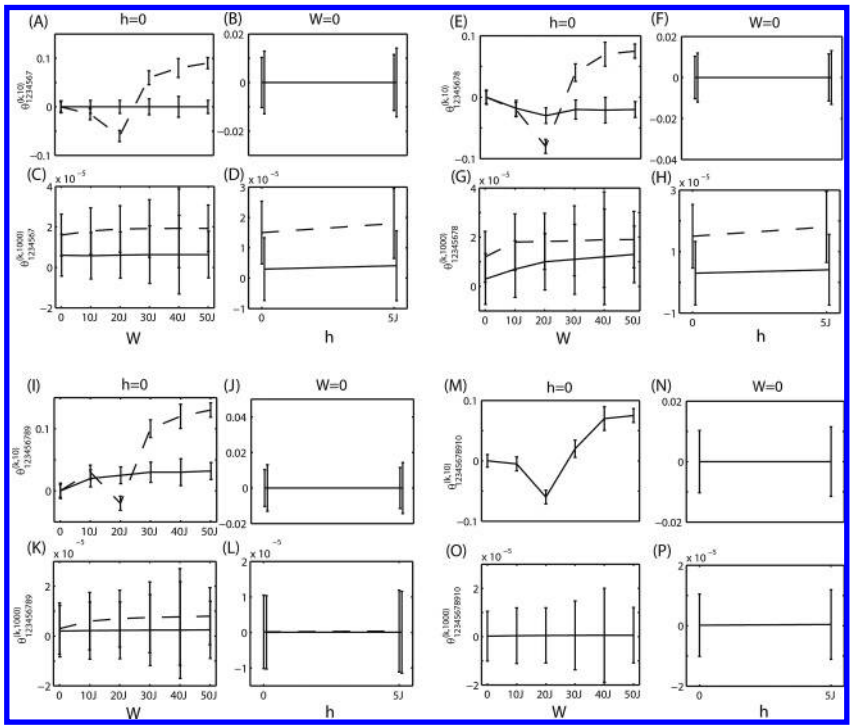

In summary, the numerical simulation demonstrated that if the size of network is sufficiently large (e.g., $N = 1000$), the influence of common and background inputs on the IG measures with three or more neuronal interactions becomes negligible even for an asymmetrically connected network. For the simulations in this section, we used $J_{ij} = 1/N + \varepsilon_{ij}$, where ε_{ij} is a random number drawn from the normal distribution $\mathrm{N}(m, \sigma^2)$ with the mean $m = 0$ and variance $\sigma^2 = 1/N$. These results suggest that the single and pairwise IG measures provide sufficient information about the network parameters as long as the asymmetry of connections is moderate.

4.3 Relationship Between the IG Measures and Asymmetry of Connections. In this section, we investigate whether the IG measures are influenced by higher asymmetry of connections.

To modify the level of asymmetry of connections, we introduced a parameter λ; asymmetric connections were set as $J_{ij} = 1/N + \lambda\varepsilon_{ij}$ where ε_{ij} is a random number drawn from the normal distribution $\mathrm{N}(m, \sigma^2)$ with the mean $m = 0$ and variance $\sigma^2 = 1/N$, respectively, and λ is an integer between 1 and 5. Note that $\lambda = 1$ corresponds to the connection setting in the previous section. Similar to the procedure in section 4.2, without

losing generality, we calculated the IG measures for a specific neuron group as follows. For the pairwise IG measure $\theta_{12}^{(k,N)}$, we selected neurons 1 and 2 and set their connection weights to $J_{12} = 1/N + \lambda\varepsilon_{12}$ and

Figure 7: Relationship between the IG measures ($\theta_{1234567}^{(k,N)}$, $\theta_{12345678}^{(k,N)}$, $\theta_{123456789}^{(k,N)}$, $\theta_{1234567890}^{(k,N)}$), a correlated input ($W$), and a background input (h) for an asymmetrically connected network. For a 10-neuron network ($N = 10$), the network parameters are set as$J = 1/10$ and $h_0 = 0.5$. For a 1000-neuron network ($N = 1000$), the network parameters are set as$J = 1/1000$ and $h_0 = 0.005$. W is sampled from 0 to 50J and h is sampled at 0 and 5J. The IG measures with the lowest LLM order (e.g., $\theta_{1234567}^{(7,10)}$) are represented by a dashed line. The IG measures with the highest LLM order (e.g., $\theta_{1234567}^{(10,10)}$) are represented by a solid line. (A) The 7-neuron IG measures for a 10-neuron network $\theta_{1234567}^{(7,10)}$ and $\theta_{1234567}^{(10,10)}$ when a correlated input (W) is varied in the absence of a background input ($h = 0$). (B) The 7-neuron IG measures for a 10-neuron network $\theta_{1234567}^{(7,10)}$ and $\theta_{1234567}^{(10,10)}$ when background input (h) is varied in the absence of a correlated input ($W = 0$). (C) The 7-neuron IG measures for a 1000-neuron network $\theta_{1234567}^{(7,1000)}$ and $\theta_{1234567}^{(10,1000)}$ when a correlated input (W) is varied in the absence of a background input ($h = 0$). (D) The 7-neuron IG measures for a 1000-neuron network $\theta_{1234567}^{(7,1000)}$ and $\theta_{1234567}^{(10,1000)}$ when background input (h) is varied in the absence of a correlated input ($W = 0$). (E) The 8-neuron IG measures for a 10-neuron network $\theta_{12345678}^{(8,10)}$ and $\theta_{12345678}^{(10,10)}$ when a correlated input (W) is varied in the absence of a background input ($h = 0$). (F) The 8-neuron IG measures for a 10-neuron network $\theta_{12345678}^{(8,10)}$ and $\theta_{12345678}^{(10,10)}$ when background input (h) is varied in the absence of a correlated input ($W = 0$). (G) The 8-neuron IG measures for a 1000-neuron network $\theta_{12345678}^{(8,1000)}$ and $\theta_{12345678}^{(10,1000)}$ when a correlated input (W) is varied in the absence of a background input ($h = 0$). (H) The 8-neuron IG measures for a 1000-neuron network $\theta_{12345678}^{(8,1000)}$ and $\theta_{12345678}^{(10,1000)}$ when background input (h) is varied in the absence of a correlated input ($W = 0$). (I) The 9-neuron IG measures for a 10-neuron network $\theta_{123456789}^{(9,10)}$ and $\theta_{123456789}^{(10,10)}$ when a correlated input (W) is varied in the absence of a background input ($h = 0$). (J) The 9-neuron IG measures for a 10-neuron network $\theta_{123456789}^{(9,10)}$ and $\theta_{123456789}^{(10,10)}$ when background input (h) is varied in the absence of a correlated input ($W = 0$). (K) The 9-neuron IG measures for a 1000-neuron network $\theta_{123456789}^{(9,1000)}$ and $\theta_{123456789}^{(10,1000)}$ when a correlated input (W) is varied in the absence of a background input ($h = 0$). (L) The 9-neuron IG measures for a 1000-neuron neuron network $\theta_{123456789}^{(9,1000)}$ and $\theta_{123456789}^{(10,1000)}$ when background input (h) is varied in the absence of a correlated input ($W = 0$). (M) The 10-neuron IG measure for a 10-neuron network $\theta_{12345678910}^{(10,10)}$ when a correlated input (W) is varied in the absence of a background input ($h = 0$). (N) The 10-neuron IG measure for a 10-neuron network $\theta_{12345678910}^{(10,10)}$ when background input (h) is varied in the absence of a correlated input ($W = 0$). (O) The 10-neuron IG measure for a 1000-neuron network $\theta_{12345678910}^{(10,1000)}$ when a correlated input (W) is varied in the absence of a background input ($h = 0$). (P) The 10-neuron IG measure for a 1000-neuron network $\theta_{12345678910}^{(10,1000)}$ when background input (h) is varied in the absence of a correlated input ($W = 0$).

$J_{21} = \frac{2}{N} - J_{12}$. In this way, the asymmetry of connections between neurons 1 and 2 was controlled by the parameter λ, but the magnitude of their total connections was kept constant ($J_{12} + J_{21} = 2/N$). The other connections were set following $J_{ij} = 1/N + \lambda\varepsilon_{ij}$. Similarly, for the three-neuron IG measure $\theta_{123}^{(k,N)}$, we selected neurons 1, 2, and 3 and set their connection weights to ($J_{12} = 1/N + \lambda\varepsilon_{12}$ and $J_{21} = 2/\mathrm{N} - J_{12}$), ($J_{23} = 1/N + \lambda\varepsilon_{23}$ and $J_{32} = 2/\mathrm{N} - J_{32}$), and ($J_{31} = 1/N + \lambda\varepsilon_{31}$ and $J_{13} = 2/\mathrm{N} - J_{31}$). The other connections were set following$J_{ij} = 1/N + \lambda\varepsilon_{ij}$. We used the same procedure for all the other IG measures with four or more neuronal interactions. We set $N = 1000$ because we are interested in the behavior of networks of biologically realistic sizes. To investigate the behavior under the influence of both common and background inputs, we used the magnitude of the common input as $W = 10J = 0.01$ and the magnitude of the background input as $h = 5J = 0.005$. The parameter m controlling the firing probability of a model neuron in equation 2.24 was set to 1. For each λ value, we performed 100 simulation trials where each trial consisted of 10^6 updates. For clarity, we show the results for the lowest and highest LLM orders only—for example, $\theta_1^{(1,1000)}$ and $\theta_1^{(10,1000)}$ for the single IG measure and $\theta_{12}^{(2,1000)}$ and $\theta_{12}^{(10,1000)}$ for the pairwise IG measure. However, we confirmed that the IG measures for all other LLM orders fell between the IG measures with the lowest and highest LLM orders. The results are reported as the mean $\pm$ SEM.

Figure 8 shows how the IG measures are influenced by the level of asymmetry of connections. The figure is organized in ascending order; the result for $\theta_1^{(k,1000)}$ is in Figure 8A, and the result for $\theta_{12345678910}^{(10,1000)}$ is in Figure 8J. Solid and gray lines represent the results for the IG measures with the lowest and highest LLM orders, respectively. We found that all the IG measures were robust against the change of asymmetry of connections in the range from $\lambda = 1$ to $\lambda = 5$ (see Figures 8A–8J). We also found that the IG measures with the highest LLM order provided the best result; for the single IG measure, $\theta_1^{(10,1000)}$ fluctuated between -2 and -1.8 (see Figure 8A, gray line). According to equation 3.1, a predicted value of $\theta_1^{(k,1000)}$ is -1.99. Figure 8A shows that $\theta_1^{(10,1000)}$ has a strong agreement with the theoretical prediction, even under a strong asymmetry of connections. Similarly, for the pairwise IG measure, $\theta_{12}^{(10,1000)}$ fluctuated around 2×10^{-3} (see Figure 8B, gray line). According to equation 3.4, the predicted value of $\theta_{12}^{(10,1000)}$ is 2×10^{-3}, which was exactly the value we found in Figure 8B. For the IG measures with three or more neuronal interactions, the IG measures with the highest LLM order ($\theta_{123}^{(10,1000)}$ to $\theta_{12345678910}^{(10,1000)}$) fluctuated around zero.

In summary, the main findings in this section are that all the IG measures are robust against the increased asymmetry of connection and that the IG measures with the highest LLM order provide the best results because they have a strong agreement with the theoretical predictions. These results suggest that the IG measures provide useful insights into the network

parameters, even for strongly asymmetric connections. The single IG measure $\theta_1^{(k,N)}$ is linearly related to a background input, and the pairwise IG measure $\theta_{12}^{(k,N)}$ is linearly related to the sum of connection weights. Furthermore, the fact that the IG measures with three or more neuronal interactions fluctuates around zero indicates that the single and pairwise IG measures contain the majority of information for the asymmetric network investigated in this letter.

5 Discussion

In this study, we investigated the influence of external inputs (a correlated input and an uncorrelated background input) and the asymmetry of connections on the IG measures beyond pairwise interactions. Our goal was two-fold. First, we aimed at finding the analytical relationships between the IG measures for up to 10-neuronal interactions and external inputs. For mathematical clarity, we investigated the dynamics of a network of 10 uniformly connected binary model neurons. By investigating the relationships in the equilibrium limit, we obtained the explicit relationship between the IG measures and the strength of correlated input W and the background input h. We confirmed that the single and pairwise IG measures were good estimators of the background input and the sum of connection weights, respectively. In contrast, for the IG measures with three or more neuronal interactions, the influence of a correlated input was stronger than a background input, and it was highly nonlinear. Second, we aimed at extending the findings for a small, uniformly connected network to an asymmetrically connected network. By numerical simulation, we found that the influence of external inputs, which was evident for a small-sized asymmetric network, became much weaker for a larger network (e.g., 1000 neurons). We also found that all the IG measures from 1-neuron to 10-neuron interactions were robust against the increased asymmetry of connections and that the IG measures with the highest LLM order provided the best result. Taken together, this investigation demonstrated that the single and pairwise IG measures were good estimators of a background input and of the sum of connection weights, even under a strong asymmetry of connections. Our study also showed that the IG measures with three or more neuronal interactions were not influenced by the network parameters if a network was sufficiently large. All of these findings support the usefulness of the IG approach and should provide further insights when the IG method is used for neural data analysis.

One of the important claims of the information-geometric approach is that the single- and pairwise-IG measures are good estimators of the background input and the sum of connection weights, respectively. In other words, the coefficients in the log-linear model can be related to the network parameters in the model. From a neuroscientific point of view, the

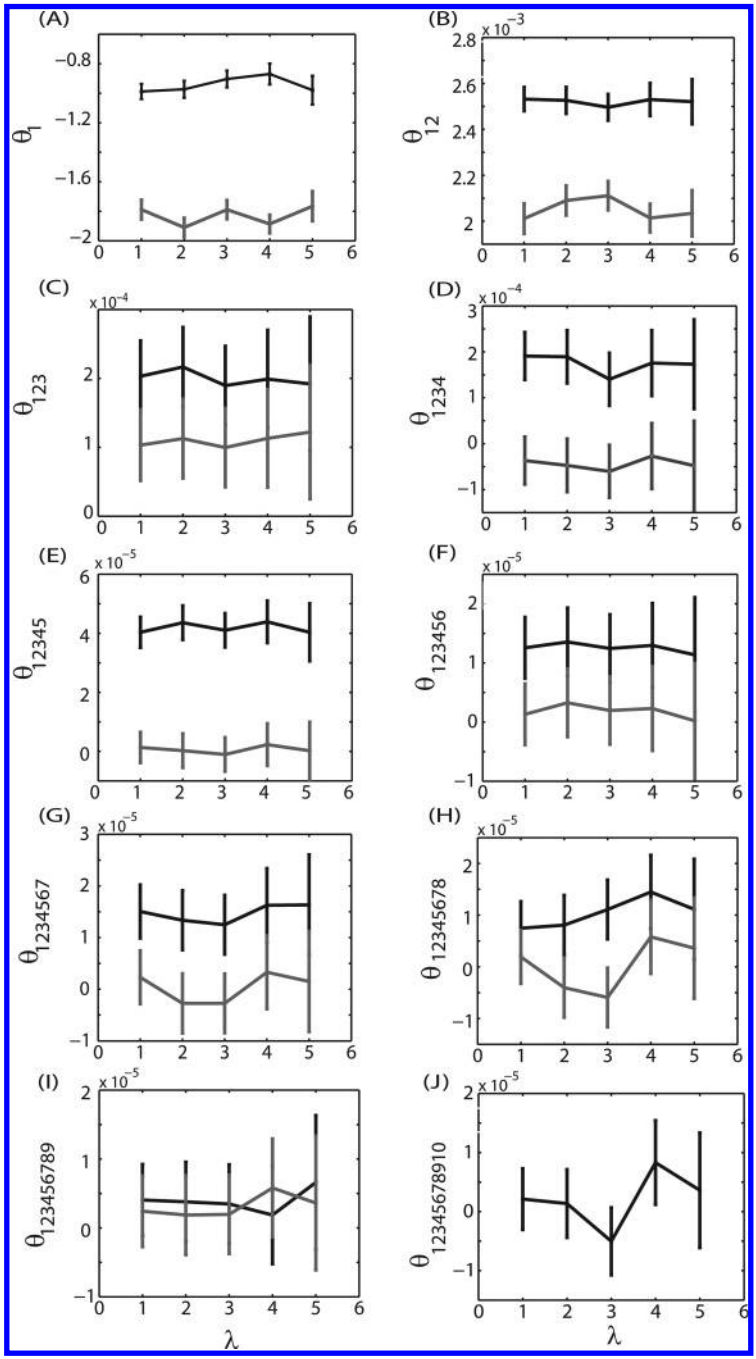
(A)
θ1
(B)
θ12
(C)
θ123
(D)
θ1234
(E)
θ12345
(F)
θ123456
(G)
θ1234567
(H)
θ12345678
(I)
θ123456789
(J)
θ12345678910
λ
λ

relationship between the pairwise IG measure and the connection weights would be particularly interesting (Schneidman, Berry, Segev, & Bialek, 2006; Tang et al., 2008; Tyler et al., 2012). However, we have to be careful as to whether the coefficients in the log-linear model actually reflect the real neuronal interaction strength. We also need to be cautious about whether the obtained complicated analytical relationship between the IG measures and external inputs is due to an oversimplified or inappropriate neural network model. We have previously investigated these questions using the Hodgkin-Huxley model (Hodgkin & Huxley, 1952). Using the NEURON simulator, we constructed a small network of cortical neurons in which each neuron was driven by an uncorrelated noisy input. The neurons were asymmetrically connected by conductance-based AMPA receptors (Hines & Carnevale, 1997; Lipa, Tatsuno, Amari, McNaughton, & Fellous, 2006; Lipa, Tatsuno, McNaughton, & Fellous, 2007). We were able to show that the pairwise IG measure was linearly related to the sum of the AMPA receptor's synaptic conductances between the neurons. In addition, we also found that the single IG measure was linearly related to the mean amplitude of noisy synaptic inputs. Recently, we have also conducted numerical simulations using a spiking neuron model (Izhikevich, 2003). One thousand cortical pyramidal neurons and 250 inhibitory neurons were connected and driven by oscillatory external inputs. We found again that the pairwise IG measure was linearly related to the sum of the connection weights (Nie, Fellous, & Tatsuno, 2014). These studies, which were conducted using more realistic

Figure 8: Relationship between the IG measures and asymmetry of connections. An integer parameter λ that controls the level of asymmetry of connections is modified between 1 and 5. The number of neurons is set to $N = 1000$, a common input is set to $W = 10J = 0.01$, and the magnitude of a background input is set to $h = 5J = 0.005$. The IG measures with the lowest LLM order (e.g., $\theta_1^{(1,1000)}$) are represented by a black line. The IG measures with the highest LLM order (e.g., $\theta_1^{(10,1000)}$) are represented by a gray line. (A) The single IG measures $\theta_1^{(1,1000)}$ and $\theta_1^{(10,1000)}$ when the asymmetry parameter (λ) is varied. (B) The pairwise IG measures $\theta_{12}^{(2,1000)}$ and $\theta_{12}^{(10,1000)}$ when the asymmetry parameter (λ) is varied. (C) The 3-neuron IG measures $\theta_{123}^{(3,1000)}$ and $\theta_{123}^{(10,1000)}$ when the asymmetry parameter (λ) is varied. (D) The 4-neuron IG measures $\theta_{1234}^{(4,1000)}$ and $\theta_{1234}^{(10,1000)}$ when the asymmetry parameter (λ) is varied. (E) The 5-neuron IG measures $\theta_{12345}^{(5,1000)}$ and $\theta_{12345}^{(10,1000)}$ when the asymmetry parameter (λ) is varied. (F) The 6-neuron IG measures $\theta_{123456}^{(6,1000)}$ and $\theta_{123456}^{(10,1000)}$ when the asymmetry parameter (λ) is varied. (G) The 7-neuron IG measures $\theta_{1234567}^{(7,1000)}$ and $\theta_{1234567}^{(10,1000)}$ when the asymmetry parameter (λ) is varied. (H) The 8-neuron IG measures $\theta_{12345678}^{(8,1000)}$ and $\theta_{12345678}^{(10,1000)}$ when the asymmetry parameter (λ) is varied. (I) The 9-neuron IG measures $\theta_{123456789}^{(9,1000)}$ and $\theta_{123456789}^{(10,1000)}$ when the asymmetry parameter (λ) is varied. (J) The 10-neuron IG measure $\theta_{12345678910}^{(10,1000)}$ when the asymmetry parameter (λ) is varied.

neuron models and synaptic connections, suggested that the coefficients in the log-linear model may be able to extract information about the real neuronal interaction strength. However, further investigation is necessary to clarify the relationship.

It is also important to note that the IG measures in this study are based on the probability of spikes counts within the same (zero-lag) time bins. The pairwise IG measure in the current form can estimate the sum of two connections as $\theta_{ij}^{(k,N)} \sim (J_{ij} + J_{ji})$ but not the directed interactions. One possible extension is to use the time-lagged IG measures. We have previously performed a preliminary study with directed connections and demonstrated that the pairwise IG measure was able to detect directed interactions (Tatsuno & Okada, 2004). Another study using a standard cross-correlogram also suggested that the effect of a directed coupling could be detected as a short latency peak or trough (Bartho et al., 2004). As the IG measure is more directly related to the connection strength than to other correlation measures such as correlation coefficient, more systematic investigation on the time-lagged IG measures should be performed in the future.

In addition, neural firing exhibits nonstationary changes in real electrophysiological experiments. The extension of our research to a time-dependent domain would be a necessary step for the analysis of real neural data (Shimazaki et al., 2012). Toward this end, we have recently investigated the property of IG measures under oscillatory inputs and found that the pairwise IG measure could estimate neural interactions (Nie et al., 2014). Finally, the proposed IG measures rely on the successful binary representation by binning spike trains. As previously discussed in Nie and Tatsuno (2012), the problem of binning needs to be treated with caution.

Despite these limitations, our study is the first effort to provide an analytical relationship between the IG measures involving up to 10 neuronal interactions and external inputs for a uniformly connected small network. It also demonstrates numerically that the IG measures are robust against the influence of external inputs and the asymmetry of connection weights if the size of the network is sufficiently large. These findings further demonstrate that the single and pairwise IG measures are robust estimators of a background input and the sum of the connection weights. We believe that this study provides useful information for the future use of IG measures. We also hope that the development of theoretical analyses, including information-geometric approaches, could lead to further insights into neural information processing.

Appendix: The Equation of the First-Order Marginal x_1 for a Ten-Neuron System

For a 10-neuron system, we solved 21 equations for 21 marginal and coincident firing variables. Below is an equation for the first-order marginal $\langle x_1 \rangle$.

The equation corresponds to equation 2.28 for a two-neuron system. Equations for other marginal and coincident firings can be written in a similar manner.

$$
\begin{aligned}
\langle x_1 \rangle = \langle x_0 x_1 x_2 x_3 x_4 x_5 x_6 x_7 x_8 x_9 \rangle \Big\{ & g(9J + W + h) - \binom{9}{1} g(8J + W + h) \\
& + \binom{9}{2} g(7J + W + h) - \binom{9}{3} g(6J + W + h) \\
& + \binom{9}{4} g(5J + W + h) - \binom{9}{5} g(4J + W + h) \\
& + \binom{9}{6} g(3J + W + h) - \binom{9}{7} g(2J + W + h) \\
& + \binom{9}{8} g(J + W + h) - \binom{9}{9} g(W + h) \\
& - \Big(g(9J + h) - \binom{9}{1} g(8J + h) + \binom{9}{2} g(7J + h) \\
& - \binom{9}{3} g(6J + h) + \binom{9}{4} g(5J + h) - \binom{9}{5} g(4J + h) \\
& + \binom{9}{6} g(3J + h) - \binom{9}{7} g(2J + h) + \binom{9}{8} g(J + h) - \binom{9}{9} g(h) \Big) \Big\} \\
& + \binom{9}{0} \langle x_1 x_2 x_3 x_4 x_5 x_6 x_7 x_8 x_9 \rangle \Big\{ g(9J + h) - \binom{9}{1} g(8J + h) \\
& + \binom{9}{2} g(7J + h) - \binom{9}{3} g(6J + h) + \binom{9}{4} g(5J + h) \\
& - \binom{9}{5} g(4J + h) + \binom{9}{6} g(3J + h) - \binom{9}{7} g(2J + h) \\
& + \binom{9}{8} g(J + h) - \binom{9}{9} g(h) \Big\} \\
& + \binom{9}{1} \langle x_0 x_1 x_2 x_3 x_4 x_5 x_6 x_7 x_8 \rangle \{ g(8J + W + h) \\
& - \binom{8}{1} g(7J + W + h) + \binom{8}{2} g(6J + W + h) \\
& - \binom{8}{3} g(5J + W + h) + \binom{8}{4} g(4J + W + h) \\
& - \binom{8}{5} g(3J + W + h) + \binom{8}{6} g(2J + W + h)
\end{aligned}
$$

$$
\begin{aligned}
&- \binom{8}{7} g(J+W+h) + \binom{8}{8} g(W+h) \\
&- \Big(g(8J+h) - \binom{8}{1} g(7J+h) + \binom{8}{2} g(6J+h) \\
&- \binom{8}{3} g(5J+h) + \binom{8}{4} g(4J+h) - \binom{8}{5} g(3J+h) \\
&+ \binom{8}{6} g(2J+h) - \binom{8}{7} g(J+h) + \binom{8}{8} g(W+h) \Big) \Big\} \\
&+ \binom{9}{1} \langle x_1 x_2 x_3 x_4 x_5 x_6 x_7 x_8 \rangle \Big\{ g(8J+h) - \binom{8}{1} g(7J+h) \\
&+ \binom{8}{2} g(6J+h) - \binom{8}{3} g(5J+h) + \binom{8}{4} g(4J+h) \\
&- \binom{8}{5} g(3J+h) + \binom{8}{6} g(2J+h) - \binom{8}{7} g(J+h) + \binom{8}{8} g(h) \Big\} \\
&+ \binom{9}{2} \langle x_0 x_1 x_2 x_3 x_4 x_5 x_6 x_7 \rangle \Big\{ g(7J+W+h) - \binom{7}{1} g(6J+W+h) \\
&+ \binom{7}{2} g(5J+W+h) - \binom{7}{3} g(4J+W+h) \\
&+ \binom{7}{4} g(3J+W+h) - \binom{7}{5} g(2J+W+h) + \binom{7}{6} g(J+W+h) \\
&- \binom{7}{7} g(W+h) - \Big(g(7J+h) - \binom{7}{1} g(6J+h) + \binom{7}{2} g(5J+h) \\
&- \binom{7}{3} g(4J+h) + \binom{7}{4} g(3J+h) - \binom{7}{5} g(2J+h) \\
&+ \binom{7}{6} g(J+h) - \binom{7}{7} g(h) \Big) \Big\} \\
&+ \binom{9}{2} \langle x_1 x_2 x_3 x_4 x_5 x_6 x_7 \rangle \Big\{ g(7J+h) - \binom{7}{1} g(6J+h) \\
&+ \binom{7}{2} g(5J+h) - \binom{7}{3} g(4J+h) + \binom{7}{4} g(3J+h) \\
&- \binom{7}{5} g(2J+h) + \binom{7}{6} g(J+h) - \binom{7}{7} g(h) \Big\} \\
&+ \binom{9}{3} \langle x_0 x_1 x_2 x_3 x_4 x_5 x_6 \rangle \Big\{ g(6J+W+h) - \binom{6}{1} g(5J+W+h)
\end{aligned}
$$

$$
\begin{aligned}
&+\binom{6}{2} g\left(4J+W+h\right)-\binom{6}{3} g\left(3J+W+h\right)+\binom{6}{4} g\left(2J+W+h\right)\\
&-\binom{6}{5} g\left(J+W+h\right)+\binom{6}{6} g\left(W+h\right)\\
&-\Bigg(g\left(6J+h\right)-\binom{6}{1} g\left(5J+h\right)+\binom{6}{2} g\left(4J+h\right)-\binom{6}{3} g\left(3J+h\right)\\
&+\binom{6}{4} g\left(2J+h\right)-\binom{6}{5} g\left(J+h\right)+\binom{6}{6} g(h)\Bigg)\Bigg\}\\
&+\binom{9}{3}\left\langle x_1x_2x_3x_4x_5x_6\right\rangle\Bigg\{g\left(6J+h\right)-\binom{6}{1} g\left(5J+h\right)\\
&+\binom{6}{2} g\left(4J+h\right)-\binom{6}{3} g\left(3J+h\right)+\binom{6}{4} g\left(2J+h\right)\\
&-\binom{6}{5} g\left(J+h\right)+\binom{6}{6} g(h)\Bigg\}\\
&+\binom{9}{4}\left\langle x_0x_1x_2x_3x_4x_5\right\rangle\Bigg\{g\left(5J+W+h\right)-\binom{5}{1} g\left(4J+W+h\right)\\
&+\binom{5}{2} g\left(3J+W+h\right)-\binom{5}{3} g\left(2J+W+h\right)+\binom{5}{4} g\left(J+W+h\right)\\
&-\binom{5}{5} g\left(W+h\right)-\Bigg(g\left(5J+h\right)-\binom{5}{1} g\left(5J+h\right)+\binom{5}{2} g\left(4J+h\right)\\
&-\binom{5}{3} g\left(3J+h\right)+\binom{5}{4} g\left(2J+h\right)-\binom{5}{5} g\left(J+h\right)\Bigg)\Bigg\}\\
&+\binom{9}{4}\left\langle x_1x_2x_3x_4x_5\right\rangle\Bigg\{g\left(5J+h\right)-\binom{5}{1} g\left(4J+h\right)+\binom{5}{2} g\left(3J+h\right)\\
&-\binom{5}{3} g\left(2J+h\right)+\binom{5}{4} g\left(J+h\right)-\binom{5}{5} g(h)\Bigg\}\\
&+\binom{9}{5}\left\langle x_0x_1x_2x_3x_4\right\rangle\Bigg\{g\left(4J+W+h\right)-\binom{4}{1} g\left(3J+W+h\right)\\
&+\binom{4}{2} g\left(2J+W+h\right)-\binom{4}{3} g\left(J+W+h\right)+\binom{4}{4} g\left(W+h\right)\\
&-\Bigg(g\left(4J+h\right)-\binom{4}{1} g\left(3J+h\right)+\binom{4}{2} g\left(2J+h\right)\\
&-\binom{4}{3} g\left(J+h\right)+\binom{4}{4} g(h)\Bigg)\Bigg\}
\end{aligned}
$$

$$
\begin{aligned}
&+\binom{9}{5}\langle x_1x_2x_3x_4\rangle\left\{g(4J+h)-\binom{4}{1}g(3J+h)+\binom{4}{2}g(2J+h)\right.\\
&\left.-\binom{4}{3}g(J+h)+\binom{4}{4}g(h)\right\}\\
&+\binom{9}{6}\langle x_0x_1x_2x_3\rangle\left\{g(3J+W+h)-\binom{3}{1}g(2J+W+h)\right.\\
&+\binom{3}{2}g(J+W+h)-\binom{3}{3}g(W+h)\\
&\left.-\left(g(3J+h)-\binom{3}{1}g(2J+h)+\binom{3}{2}g(J+h)-\binom{3}{3}g(h)\right)\right\}\\
&+\binom{9}{6}\langle x_1x_2x_3\rangle\left\{g(3J+h)-\binom{3}{1}g(2J+h)\right.\\
&\left.+\binom{3}{2}g(J+h)-\binom{3}{3}g(h)\right\}\\
&+\binom{9}{7}\langle x_0x_1x_2\rangle\left\{g(2J+W+h)-\binom{2}{1}g(J+W+h)\right.\\
&\left.+\binom{2}{2}g(W+h)-\left(g(2J+h)-\binom{2}{1}g(J+h)+\binom{2}{2}g(h)\right)\right\}\\
&+\binom{9}{7}\langle x_1x_2\rangle\left\{g(2J+h)-\binom{2}{1}g(J+h)+\binom{2}{2}g(h)\right\}\\
&+\binom{9}{8}\langle x_0x_1\rangle\{g(J+W+h)-g(W+h)-(g(J+h)-g(h))\}\\
&+\binom{9}{8}\langle x_1\rangle\{g(J+h)-g(h)\}+\binom{9}{9}\langle x_0\rangle\{g(W+h)-g(h)\}+g(h)
\end{aligned}
$$

Acknowledgments

We thank Amanda Mauthe-Kaddoura for proofreading this manuscript. We also thank anonymous reviewers for their helpful comments and suggestions. This work was supported by Alberta Innovates Technology Futures (SCH001), the National Science Foundation (CRCNS-1010172), and Alberta Innovates Health Solutions (Polaris Award).

References

Abeles, M., & Gerstein, G. L. (1988). Detecting spatiotemporal firing patterns among simultaneously recorded single neurons. *J. Neurophysiol.*, *60*(3), 909–924.

Aertsen, A. M., Gerstein, G. L., Habib, M. K., & Palm, G. (1989). Dynamics of neuronal firing correlation: Modulation of "effective connectivity." *J. Neurophysiol.*, *61*(5), 900–917.

Amari, S. (2001). Information geometry on hierarchy of probability distributions. *IEEE Transactions on Information Theory*, *47*(5), 1701–1711.

Amari, S. (2009). Measure of correlation orthogonal to change in firing rate. *Neural Comput.*, *21*(4), 960–972.

Amari, S., & Nagaoka, H. (2000). *Methods of information geometry*. New York: Oxford University Press.

Amari, S., Nakahara, H., Wu, S., & Sakai, Y. (2003). Synchronous firing and higher-order interactions in neuron pool. *Neural Comput.*, *15*(1), 127–142.

Bartho, P., Hirase, H., Monconduit, L., Zugaro, M., Harris, K., & Buzsaki, G. (2004). Characterization of neocortical principal cells and interneurons by network interactions and extracellular features. *J. Neurophysiol.*, *92*, 600–608.

Brown, E. N., Kass, R. E., & Mitra, P. P. (2004). Multiple neural spike train data analysis: state-of-the-art and future challenges. *Nat. Neurosci.*, *7*(5), 456–461.

Czanner, G., Grün, S., & Iyengar, S. (2005). Theory of the snowflake plot and its relations to higher-order analysis methods. *Neural Comput.*, *17*(7), 1456–1479.

Eleuteri, A., Tagliaferri, R., & Milano, L. (2005). A novel information geometric approach to variable selection in MLP networks. *Neural Netw.*, *18*(10), 1309–1318.

Fellous, J. M., Tiesinga, P. H., Thomas, P. J., & Sejnowski, T. J. (2004). Discovering spike patterns in neuronal responses. *J. Neurosci.*, *24*(12), 2989–3001.

Ganmor, E., Segev, R., & Schneidman, E. (2011). Sparse low-order interaction network underlies a highly correlated and learnable neural population code. *Proc. Natl. Acad. Sci. USA*, *108*(23), 9679–9684.

Gerstein, G. L., & Perkel, D. H. (1969). Simultaneously recorded trains of action potentials: Analysis and functional interpretation. *Science*, *164*(881), 828–830.

Ginzburg, I. I., & Sompolinsky, H. (1994). Theory of correlations in stochastic neural networks. *Physical Review. E. Statistical Physics, Plasmas, Fluids, and Related Interdisciplinary Topics*, *50*(4), 3171–3191.

Grün, S., Diesmann, M., & Aertsen, A. (2002a). Unitary events in multiple single-neuron spiking activity: I. Detection and significance. *Neural Comput.*, *14*(1), 43–80.

Grün, S., Diesmann, M., & Aertsen, A. (2002b). Unitary events in multiple single-neuron spiking activity: II. Nonstationary data. *Neural Comput.*, *14*(1), 81–119.

Hines, M. L., & Carnevale, N. T. (1997). The NEURON simulation environment. *Neural Comput.*, *9*(6), 1179–1209.

Hodgkin, A. L., & Huxley, A. F. (1952). A quantitative description of membrane current and its application to conduction and excitation in nerve. *J. Physiol.*, *117*(4), 500–544.

Ikeda, K. (2005). Information geometry of interspike intervals in spiking neurons. *Neural Comput.*, *17*(12), 2719–2735.

Ince, R. A., Senatore, R., Arabzadeh, E., Montani, F., Diamond, M. E., & Panzeri, S. (2010). Information-theoretic methods for studying population codes. *Neural Netw.*, *23*(6), 713–727.

Izhikevich, E. M. (2003). Simple model of spiking neurons. *IEEE Trans. Neural Netw.*, *14*(6), 1569–1572.

Lipa, P., Tatsuno, M., Amari, S., McNaughton, B. L., & Fellous, J. M. (2006). A novel analysis framework for characterizing ensemble spike patterns using spike train clustering and information geometry. *Soc. Neurosci. Abstr.*, *36.371*, 6.

Lipa, P., Tatsuno, M., McNaughton, B. L., & Fellous, J. M. (2007). Dynamics of neural assemblies involved in memory-trace replay. *Soc. Neurosci. Abstr.*, *37.308*, 13.

Lopes-dos-Santos, V., Conde-Ocazionez, S., Nicolelis, M. A., Ribeiro, S. T., & Tort, A. B. (2011). Neuronal assembly detection and cell membership specification by principal component analysis. *PLoS One*, *6*(6), e20996.

Miura, K., Okada, M., & Amari, S. (2006). Estimating spiking irregularities under changing environments. *Neural Comput.*, *18*(10), 2359–2386.

Nakahara, H., & Amari, S. (2002). Information-geometric measure for neural spikes. *Neural Comput.*, *14*(10), 2269–2316.

Nakahara, H., Amari, S., & Richmond, B. J. (2006). A comparison of descriptive models of a single spike train by information-geometric measure. *Neural Comput.*, *18*(3), 545–568.

Nie, Y., Fellous, J. M., & Tatsuno, M. (2014). Information-geometric measures estimate neural interactions during oscillatory brain states. *Frontiers in Neural Circuits*, *8*, 11. doi: 10.3389/fncir.2014.00013

Nie, Y., & Tatsuno, M. (2012). Information-geometric measures for estimation of connection weight under correlated inputs. *Neural Comput.*, *12*, 3213–3245.

Ohiorhenuan, I. E., Mechler, F., Purpura, K. P., Schmid, A. M., Hu, Q., & Victor, J. D. (2010). Sparse coding and high-order correlations in fine-scale cortical networks. *Nature*, *466*(7306), 617–621.

Ohiorhenuan, I. E., & Victor, J. D. (2011). Information-geometric measure of 3-neuron firing patterns characterizes scale-dependence in cortical networks. *J. Comput. Neurosci.*, *30*(1), 125–141.

Panzeri, S., & Schultz, S. R. (2001). A unified approach to the study of temporal, correlational, and rate coding. *Neural Comput.*, *13*(6), 1311–1349.

Peyrache, A., Benchenane, K., Khamassi, M., Wiener, S. I., & Battaglia, F. P. (2009). Principal component analysis of ensemble recordings reveals cell assemblies at high temporal resolution. *J. Comput. Neurosci.*, *29*, 309–325.

Schneidman, E., Berry, M. J., Segev II, R., & Bialek, W. (2006). Weak pairwise correlations imply strongly correlated network states in a neural population. *Nature*, *440*(7087), 1007–1012.

Shimazaki, H., Amari, S., Brown, E. N., & Grün, S. (2012). State-space analysis of time-varying higher-order spike correlation for multiple neural spike train data. *PLoS Computational Biology*, *8*(3), e1002385.

Shimazaki, H., & Shinomoto, S. (2007). A method for selecting the bin size of a time histogram. *Neural Comput.*, *19*(6), 1503–1527.

Shimokawa, T., & Shinomoto, S. (2009). Estimating instantaneous irregularity of neuronal firing. *Neural Comput.*, *21*(7), 1931–1951.

Tang, A., Jackson, D., Hobbs, J., Chen, W., Smith, J. L., Patel, H., . . . Beggs, J. M. (2008). A maximum entropy model applied to spatial and temporal correlations from cortical networks in vitro. *J. Neurosci.*, *28*(2), 505–518.

Tatsuno, M., Fellous, J. M., & Amari, S. I. (2009). Information-geometric measures as robust estimators of connection strengths and external inputs. *Neural Comput.*, *21*(8), 2309–2335.

Tatsuno, M., & Okada, M. (2004). Investigation of possible neural architectures underlying information-geometric measures. *Neural Comput.*, *16*(4), 737–765.

Tyler, A. L., Mahoney, J. M., Richard, G. R., Holmes, G. L., Lenck-Santini, P. P., & Scott, R. C. (2012). Functional network changes in hippocampal CA1 after status epilepticus predict spatial memory deficits in rats. *Journal of Neuroscience*, *32*(33), 11365–11376.

Urban, N. N., Henze, D. A., & Barrionuevo, G. (2001). Revisiting the role of the hippocampal mossy fiber synapse. *Hippocampus*, *11*(4), 408–417.

Zhang, K., Ginzburg, I., McNaughton, B. L., & Sejnowski, T. J. (1998). Interpreting neuronal population activity by reconstruction: Unified framework with application to hippocampal place cells. *J. Neurophysiol.*, *79*(2), 1017–1044.

Received February 20, 2013; accepted April 15, 2014.